AN ABSTRACT OF THE THESIS OF

MING J. KONG (Name) for the degree MASTER OF SCIENCE (Degree)

in CHEMISTRY (Analytical) (Major Department) presented on 30 August 1974 (Date)

Title: DIFFUSION IN SILICONE POLYMERS

Redacted for privacy

Abstract approved: Stephen J. Hawkes

The study of diffusion coefficients of n-alkanes and other organic compounds in silicones is undertaken by gas-liquid chromatography. About 0.3% of stationary phase is coated on glass bead support so that the only significant source of peak spreading is due to slow liquid phase mass transfer.

Diffusion coefficients are higher in higher molecular weight methylsilicones than in lower molecular weight. The anomaly is partially explained by the increase of free volume with increasing molecular weight. Partition coefficients of n-alkanes in the methylsilicones are independent of the molecular weights of the silicones. Chromatographic peaks for n-alkanes in methylsilicones become increasingly skewed as the molecular weight of the n-alkane increases. Diffusion coefficients in phenyl, fluoro and cyanosilicones are strongly dependent on the steric hindrance of the substituent groups of the silicones and the molecular size and shape of the penetrants.

Three equations for the dependence of the diffusion coefficients of n-alkanes on the physical properties of the penetrant-polymer system are investigated by linear regression. It is found that the best fit through the 158 data points is obtained when the densities and the percent phenyl content of silicones are included in the regression equation. It suggests the diffusion process is dependent on the free volume and steric hindrance of the silicones studied, and is independent of intermolecular attraction between the polymer and the penetrant.

Diffusion in Silicone Polymers

by

Ming J. Kong

A THESIS

submitted to

Oregon State University

in partial fulfillment of
the requirements for the
degree of

Master of Science

Completed August 1974

Commencement June 1975

APPROVED:

Redacted for privacy

Associate Professor of Chemistry
in charge of major

Redacted for privacy

Head of Department of Chemistry

Redacted for privacy

Dean of Graduate School

Date thesis is presented August 30, 1974

Typed by Mary Jo Stratton for Ming J. Kong

ACKNOWLEDGMENTS

The author wishes to express his appreciation to Dr. Stephen J. Hawkes for his constant encouragement, advice, and assistance throughout the course of this research and preparation of the thesis.

Appreciation is also due to Drs. Harry Freund and Frank J. F. Yang for their valuable suggestions with this research.

The financial support of research grant GP-15430 from the National Science Foundation is acknowledged.

Finally, the author is indebted to his parents for their constant encouragement which made this study possible.

TABLE OF CONTENTS

	Page
I. INTRODUCTION	1
II. CHEMISTRY OF SILICONES	2
Nomenclature	2
Methylsilicones	4
Phenylsilicones	4
Fluoroalkylsilicones	5
Cyanoalkylsilicones	5
III. THEORY OF CHROMATOGRAPHY	6
Flow Phenomenon	6
Longitudinal Molecular Diffusion	7
Diffusion in the Stationary Phase	8
Gas Phase Mass Transfer	10
Glass Bead Support	14
IV. EXPERIMENTAL	16
Apparatus	16
Procedure	16
Chromatographic Procedure	17
Calculations	18
V. RESULTS AND DISCUSSION	20
Diffusion Coefficients	20
Methylsilicones	20
Phenylsilicones	24
Fluorosilicones	25
Cyanosilicone	25
Partition Coefficients	26
Methylsilicones	26
Phenylsilicones	27
Fluorosilicones	27
Cyanosilicone	27

Page

VI. PHILOSOPHY 29

Diffusion in Polydimethylsiloxanes 29
Translational Friction Coefficients and Comparison with Monomeric Friction Coefficients of Polymer Segments 29
Diffusion in Phenylsilicones, Fluorosilicones, and Cyanosilicones 32

VII. STATISTICAL LINEAR REGRESSION MODELS FOR DIFFUSION OF n-ALKANES IN SILICONES 34

VIII. COMMENTS ON THE DETERMINATION OF DIFFUSION COEFFICIENTS BY GAS-LIQUID CHROMATOGRAPHY 38

BIBLIOGRAPHY 40

APPENDIX 44

LIST OF FIGURES

Figure		Page
1	Structure of silicones.	44
2	Log diffusion coefficients against log partition coefficients in methylsilicones at 50 ± 2°C.	46
3	Log diffusion coefficients against log partition coefficients in methylsilicones at 99 ± 3°C.	47
4	Log diffusion coefficients against log partition coefficients in methylsilicones at 148 ± 3°C.	48
5	Log diffusion coefficients against log partition coefficients in methylsilicones at 197.8 ± 0.3°C.	49
6	Diffusion coefficients against log partition coefficients in phenyl- and fluorosilicones at 49 ± 2°C.	50
7	Diffusion coefficients against log partition coefficients in phenyl-, fluoro- and cyano-silicones at 98 ± 2°C.	51
8	Diffusion coefficients against log partition coefficients in phenyl-, fluoro- and cyano-silicones at 149 ± 1°C.	52
9	Diffusion coefficients against log partition coefficients in phenyl-, fluoro- and cyano-silicones at 197 ± 3°C and 246 ± 2°C.	53
10	Diffusion of benzene in polydimethylsiloxanes.	54
11	Differential of ratio of specific volume at temperature T to specific volume at 25°C with respect to temperature for PDMS (mol. wt. 10^5) and DC-200.	55
12	Theoretical ln D_s against experimental ln D_s -- regression equation 26.	56

Figure		Page
13	Diffusion coefficients against percent phenyl content of phenylsilicones at 149 $\pm$ 1°C.	57
14	Theoretical ln D_s against experimental ln D_s--regression equation 30.	58

LIST OF TABLES

Table		Page
1	Some properties of silicones.	59
2	Column characteristics.	60
3	D_o of n-alkanes and aromatics.	61
4	Diffusion coefficients in cm^2/sec and partition coefficients of n-alkanes and aromatics in methylsilicones at $50 \pm 2^{\circ}C$.	62
5	Diffusion coefficients in cm^2/sec and partition coefficients of n-alkanes and aromatics in methylsilicones at $99 \pm 3^{\circ}C$.	63
6	Diffusion coefficients in cm^2/sec and partition coefficients of n-alkanes and aromatics in methylsilicones at $148 \pm 3^{\circ}C$.	64
7	Diffusion coefficients in cm^2/sec and partition coefficients of n-alkanes and aromatics in methylsilicones at $197.8 \pm 0.3^{\circ}C$ and $239^{\circ}C$.	65
8	Diffusion coefficients in cm^2/sec and partition coefficients of n-alkanes and aromatics in phenyl- and fluorosilicones at $49 \pm 2^{\circ}C$.	66
9	Diffusion coefficients in cm^2/sec and partition coefficients of n-alkanes and aromatics in phenyl-, fluoro- and cyanosilicones at $98 \pm 2^{\circ}C$.	67
10	Diffusion coefficients in cm^2/sec and partition coefficients in n-alkanes and aromatics in phenyl-, fluoro- and cyanosilicones at $149 \pm 1^{\circ}C$.	68
11	Diffusion coefficients in cm^2/sec and partition coefficients of n-alkanes and aromatics in phenyl-, fluoro- and cyanosilicones at $197 \pm 3^{\circ}C$.	69

Table		Page
12	Diffusion coefficients in cm^2/sec and partition coefficients of n-alkanes and aromatics in phenyl-, fluoro- and cyanosilicones at 246 $\pm$ 2°C.	70
13	Translational friction coefficients for benzene and monomeric friction coefficients for segmental motion.	71
14	Ratio of specific volume at temperature T to specific volume at 25°C for PDMS (mol. wt. 10^5) at selected temperatures.	72
15	Ratio of volume at temperature T to volume at 25°C for DC-200 at selected temperatures.	73
16	Regression equations for diffusion coefficients of n-alkanes in individual silicone.	74
17	Regression equations for diffusion coefficients of n-alkanes in silicones.	75

DIFFUSION IN SILICONE POLYMERS

I. INTRODUCTION

Since James and Martin (1) employed a commercially available silicone as the stationary phase in their pioneering gas chromatographic works, a considerable number of polysiloxanes of various polarity have been used. Most work on liquid stationary phases has concentrated on their partition properties and their thermal stability with very little attention to their diffusional properties and the effect on zone broadening. At a time when standardization of stationary phases is being actively pursued, it is essential to have some information on this subject.

Diffusion in polymers is a process by which matter is transported from one portion of a polymer to another portion. The diffusion process has a strong dependence on the polymer density and the molecular diameter of the penetrant molecule (2, 3). A particular goal of this research is to establish diffusion models in silicone polymers.

II. CHEMISTRY OF SILICONES

Nomenclature

For the purpose of simplification and understanding of the language of the chemistry of silicones, the following is presented to show the symbols and formulae used in discussing silicones:

Symbol	Structural Formula	Functionality
M	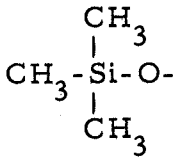	monofunctional or end-blocker
D	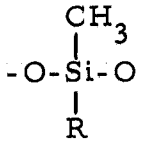	difunctional or backbone

where R represents organofunctional groups.

As an example of the use of the symbols, D_4 would represent the following structure:

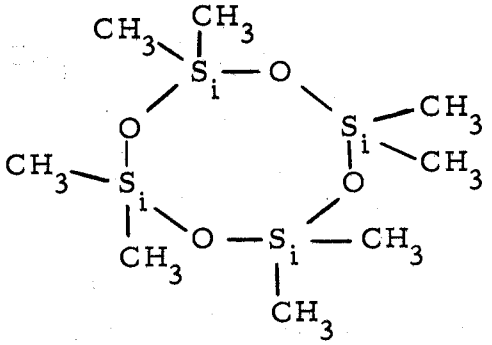

Chemically, silicones are quite different from all other materials. This difference in chemical structure begins with the atomic backbone of silicone fluids. Silicone fluids have a backbone of silicon-oxygen linkages. It is this Si-O linkage that contributes to the outstanding high temperature characteristics and general inertness of silicone fluids. The presence of oxygen in siloxane polymer spaces the units to provide greater freedom for bending than is possible in the polysilane (4).

Rotational freedom in siloxane bonds is a second fundamental phenomenon. Roth (5, 6) indicated that electron diffraction data could not be reconciled without assuming that the methyl group swept out a large umbrella-like surface as though oscillating with a large amplitude at a fixed radius. He concluded that this indicates an extreme freedom of rotation about the siloxane bond.

The siloxane bond may be broken rather easily by certain reagents such as acids, chlorosilanes, or antimony pentachloride (7, 8, 9). This indicates the labile nature of the siloxane bond which may be attributed to the large ionic character of the bond. Pauling (10) suggests the value of 50%, while Hannay and Smyth (11) set a new standard for ionic character of bonds which yield for Si-O the value of 37%.

Methylsilicones

Methylsilicones are widely used in chromatography because of their good temperature stability and their essentially nonpolar separating characteristics. The S. G. of methylsilicones are less than that of water. Surface tension of silicone fluids is unusually low, resulting in great spreading power of silicone fluids on the solid support. The methylsilicones are stable in the absence of oxygen, as in a GC column. GC Grade SE-30 may be used for extended periods of time at 350°C (12). Any bleeding which does occur under this condition will usually indicate the decomposition of the polymer chain to the smaller cyclic species (D_x), where x is a non-zero positive integer.

Phenylsilicones

Phenylsilicones cover a wide range of phenyl contents and molecular weights. The Dow Corning fluids DC-550 (25% phenyl), and DC-710 (50% phenyl) contain methylphenylsiloxy units. These low molecular weight polymers contain relatively large amounts of volatiles which can be removed by vacuum stripping at high temperature. The phenylsilicones have thermal stabilities somewhat higher than the methylsilicones (13).

Fluoroalkylsilicones

All fluoroalkylsilicones currently available are homopolymers of (3, 3, 3-trifluoropropyl) methyl, such as Ohio Valley's OV-210, and Supelco's low molecular weight SP-2401. Thermogravimetric analyses run from 200° to 300°C at a heat rate of 2°/min in a helium atmosphere show that SP-2401 has a smaller percent weight loss than OV-210 (14).

Cyanoalkylsilicones

Silicone oils containing cyanopropyl groups were offered as a new class of polar stationary phases by Roszsche in 1962 (15, 16). By varying the number of cyanopropyl groups, phases of varying polarity were produced. OV-225 (25% γ cyanopropyl-25% phenyl) is a copolymer of (γ cyanopropyl) methyl and methylphenyl (15). O. V. now offers OV-275 which has the highest cyano-content of any available silicone.

The physical properties and structures of the ten silicone polymers investigated in this work are listed in Table 1 (17, 18, 19 and 20) and Figure 1, respectively.

III. THEORY OF CHROMATOGRAPHY

The measure of zone dispersion in a chromatographic system is given as

$$H = \frac{d\,\sigma^2}{d\,L} \tag{1}$$

where $d\,\sigma^2$ = incremental variance

$d\,L$ = incremental length of column

H is called "height equivalent to a theoretical plate" (HETP) for historic reasons. A more workable expression is

$$H = \frac{\sigma^2}{L} \tag{2}$$

where sufficient homogeneity of the column is assumed. Variances are additive provided that the variances of the separate mechanisms are not interactive. Hence, the variances from various dispersion mechanisms can be summed to a total variance.

$$\sigma^2 = \sigma_1^2 + \sigma_2^2 + \sigma_3^2 + \ldots \tag{3}$$

Flow Phenomenon

The flow streamlines in a bed of granular particles veer tortuously back and forth in an effort to find relatively unobstructed pathways for fluid flow. Some molecules, by following relatively open

pathways, may acquire a greater than average downstream velocity, and others may become enmeshed in restricted channels and lag behind. The net result is zone dispersion and this effect is usually called eddy diffusion in the chromatographic literature. The zone dispersion caused by eddy diffusion is proportional to the diameter of the particle.

$$H = 2 \lambda_i d_p \tag{4}$$

where λ_i = eddy diffusion coefficient

d_p = mean particle diameter

Longitudinal Molecular Diffusion

Longitudinal molecular diffusion is a random molecular diffusion process in the direction of flow in the mobile phase. Molecular diffusion gives a contribution inversely proportional to the flow velocity because the higher the velocity the less time there is for diffusion to take place. In packed columns the tortuous and constricted path needed by molecules to skirt the granules reduces the actual distance diffused, and an obstructive factor γ, slightly less than unity, is applicable. The plate height contribution is therefore

$$H = \frac{2 \gamma D_m}{v} \tag{5}$$

where γ = obstruction factor

D_m = molecular diffusion coefficient of the solute in the mobile phase

v = mean velocity of the mobile phase

The obstruction factor is the ratio of the direct-line distance between two points in a packed column to the actual distance a molecule must travel around the particles.

Under some circumstances, longitudinal diffusion in the stationary phase also contributes a plate height (21).

$$H = \frac{2 \gamma_s D_s}{v} \quad \frac{(1 - R)}{R} \tag{6}$$

where γ_s and D_s are the obstruction factor and molecular diffusion coefficient of the solute in the stationary phase. R is the retention ratio, or equivalently, the fraction of solute in the mobile phase. For all gas chromatographic columns, equation (5) is the major contribution.

Diffusion in the Stationary Phase

Zone dispersion is largely a result of various nonequilibrium processes controlled by liquid diffusion and gaseous diffusion. With heavily loaded columns, the slowness of liquid diffusion makes this term rate-controlling.

The bulk of the liquid phase in gas chromatography may be considered to occupy the cavities or pores of the solid support.

Between these isolated liquid pools is a thin film of liquid held to the solid by adsorption forces. As the chromatographic zone passes through each region the liquid pools first absorb solute, then release it back into the gas stream. At any given moment there is a certain flux of solute across the boundaries of a particular pool. Most of this flux typically occurs through the gas-liquid interface. Very little of it occurs through the thin film connecting one pool to another because of the film's dimension. Virtually none of the flux occurs through the liquid-solid interface because of the solid's impermeability. The combination law for the resistance to mass transfer in the stationary phase suggested by Giddings (22) is

$$H = \Sigma\, q_j \, \frac{V_j}{V_s} \, R\,(1-R) \, \frac{d_j^2 v}{D_s} \qquad (7)$$

where q_j = configuration factor

$\frac{V_j}{V_s}$ = volume in unit j relative to the entire stationary phase volume

d_j = maximum depth of the unit from its open surface

The expression indicates that the dispersion may be written as a sum of terms, each a function solely of the configuration of a given unit of liquid. The dimensionless quantity q_j is usually within an order of magnitude of unity. In glass bead columns in gas chromatography

where the liquid units all occupy the "pores" around the bead contact points, there is only one kind of unit composing the total stationary phase. The plate height contribution reduces to

$$H = qR\,(1-R)\,\frac{d^2 v}{D_s} \tag{8}$$

Giddings has assumed a unit of stationary phase is a narrow spike and derived the configuration factor q (21).

$$q = 2/(n+1)\,(n+3) \tag{9}$$

where $n \geq 0$ by physical arguments. The plate height may consequently be expressed as

$$H = \frac{2}{(n+1)\,(n+3)}\,R(1-R)\,\frac{d^2 v}{D_s} \tag{10}$$

If small amounts of liquid are used in the glass bead columns, the liquid regions are mathematically equivalent to narrow pores with $n = 3$.

Gas Phase Mass Transfer

Mobile phase zone dispersion arises in a column because lateral diffusion among the flow paths are non-instantaneous. The diffusive exchange leads to plate height expression (21)

$$H = \omega_i\, d_p^2\, v\, /\, D_m \tag{11}$$

where D_m = diffusion coefficient in the mobile phase

where ω_i = coefficient of mobile phase plate height contribution of the order of unity

Giddings (23) has pointed out that eddy diffusion and lateral mass transfer in the mobile phase actually couple and reduce the dispersion. Knox (24) investigated the spreading of bands of potassium permanganate in aqueous 10% potassium nitrate solution during elution through columns packed with glass beads. This experiment provided conclusive evidence for the coupling of eddy diffusion and transverse diffusion processes over a 10,000-fold range of reduced fluid velocity.

The final plate height term is

$$H = \left[1/2\ \lambda_i d_p + D_m/\omega_i d_p^2 v\right]^{-1} + 2\gamma D_m/v + \frac{2}{(n+1)(n+3)} R(1-R) \frac{d^2 v}{D_s} \qquad (12)$$

The flow mechanism does not become dominant until the reduced velocity (equation 17) exceeds about 40, much higher than the practical operating range in gas chromatography (21).

With a highly-loaded column, the contribution to the spreading of the eluted zone by gas phase mass transfer is small in comparison with that contributed by the liquid phase mass transfer at fast flow velocity (25). Hence, the gas phase mass transfer is neglected in the calculation of the diffusion coefficients in this work. For gas-liquid

glass beads chromatographic columns, the plate height dispersion term is

$$H = \frac{2 \gamma D_{g1} jf}{v P_o} + \frac{k d_p^2 v}{120 D_s (1+k)^2} \left[\frac{\% \rho_g}{3 m \rho_\ell} \right]^{1/2} \qquad (13)$$

where D_{g1} = diffusivity of sample in the mobile phase at unit pressure, cm^2/sec

j = James-Martin compressibility factor, $3(P^2 - 1)/2(P^3 - 1)$

f = Gidding's compressibility factor, $\frac{9(P^4 - 1)(P^2 - 1)}{8(P^3 - 1)^2}$

P = ratio of inlet to outlet pressure

P_o = outlet pressure in atmosphere

$\%$ = percentage of stationary phase on glass beads

ρ_g = density of glass, gm/cm^3

ρ_ℓ = density of solvent, gm/cm^3

m = number of contact points per bead, 6.25

k = ratio of mass of solute in stationary and mobile phases

The quantity d^2 is obtained as $(2r^2/5)(\% \rho_g/3m \rho_\ell)^{1/2}$ where r is the mean bead radius. The quantity

$$\frac{k d_p^2}{120 D_s (1+k)^2} \left[\frac{\% \rho_g}{3 m \rho_\ell} \right]^{1/2}$$

is known as C_1 in chromatographic literature. This term was suggested by Giddings (26), and its validity was experimentally verified (25, 27). The retention ratio, R, is numerically equal to $1/(1+k)$.

The column capacity ratio is defined as

$$k = K\left(\frac{V_l}{V_g}\right) \tag{14}$$

where K = partition coefficient

V_l = total volume in column of stationary phase

V_g = total volume in column of mobile phase

The partition coefficient is the ratio of the concentrations in mass/volume of a partitioned sample in the two phases. The column capacity is a parameter dependent on column conditions and may be obtained experimentally as

$$k = \frac{t_r - t_o}{t_o} \tag{15}$$

where t_r = total retention time of sorbed sample

t_o = total retention time of unsorbed sample

The interstitial velocity, v, is the time-averaged velocity

$$v = \frac{L}{t_o} \tag{16}$$

where L = length of the column

t_o = elution time of unretained sample

The reduced velocity, ν, is defined as

$$\nu = v d_p / D_m \tag{17}$$

The plate height of a sample eluted out of a chromatographic column can be obtained as

$$H = \frac{L}{5.5452} \left(\frac{w_{1/2}}{t_r}\right)^2 \tag{18}$$

where $w_{1/2}$ = width of the sample peak at half-height

Equation (18) is derived with the assumption that the sample peak is Gaussian.

At sufficiently high velocity the longitudinal molecular diffusion in equation (13) becomes small (about 10% of the total dispersion) when compared with that of the liquid phase mass transfer. The C_1 term depends on the time a solute molecule spends in the liquid phase and the time is a function of the following:

1. The film thickness, which is dependent on the amount of liquid as well as solid interaction which control the distribution of the liquid on the support.
2. The diffusivity of the solute sample in the liquid phase.
3. The sample retention time.

Glass Bead Support

In order to study the effect of liquid loading on column

efficiency, one requires to use a support whose geometry is known. Glass beads are used due to the well defined geometry and the low porosity of the beads. The geometry of the liquid phase in gas-liquid phase is profoundly important because it governs the rate of mass transfer through the liquid and its depth. The correlation of support and liquid distribution is defined by the study of forces holding the liquid to the support. Any liquid added to a wettable solid is subjected to both adsorption and capillary forces (28, 29). The intermolecular attraction of solid and liquid leads to adsorption and the liquid-liquid intermolecular attraction is responsible for surface tension and leads to capillary condensation in pores or around contact points (30). Adsorption forces, when predominant, give a rather uniform film thinly distributed over the available surface, and hence the column is efficient (C_1 term is small). Capillary forces, when predominant, collect the liquid into pools around the contact points, and hence the column is inefficient. According to Giddings, the interaction between solid and liquid is very weak and in most practical cases the liquid distribution will be controlled by capillary condensation into the contact points.

IV. EXPERIMENTAL

Apparatus

A Perkin-Elmer F-11 gas chromatograph was adapted for this work. A Carle thermistor detector was used. The injection system was a Swagelok T with the carrier gas inlet connected to one end and the loaded column to the other end. A silicone rubber septum was used as the injection point. The columns were approximately 6 feet long, 1/4 in. O.D. coiled copper tubes packed with polymer-coated 60/80 mesh Ballotini glass beads. The packed columns were sealed with wire screen. Peaks were recorded on an Esterline Angus E 1101S recorder with a full-scale deflection time of 0.2 sec.

Procedure

The Ballotini beads were obtained from VWR. They were chosen for study because they were previously found to be more nearly spherical than other brands (25, 31), and are less expensive. Sieving the beads was difficult since they clogged the pores of the sieve firmly and often permanently. Accordingly, the bottoms of the sieves needed to be brushed frequently. After sieving, the beads were cleaned with conc. HCl, water, acetone, and ether to remove any inorganic contaminations.

Accurately weighed silicone was dissolved in a suitable solvent in a beaker. Sufficient amount of glass beads was added to the silicone solution that the percent of silicone was approximately 0.3. The resultant mixture was stirred and heated on a hot plate continuously until all solvent was vaporized. The coated glass beads were then packed into a 6 ft long, 1/4 in. O.D. copper column by pushing them with a stirring rod through a small funnel. The funnel was connected to the column with a 1 in. tygon tubing.

Since the silicone adhered to the walls of the beaker and the funnel, the original loading of beads was not the same as that in the column. The excess coated glass beads were boiled with solvent to dissolve the unused silicone. The funnel was rinsed with boiling solvent to remove adhered silicone. The glass beads and silicone were separated by filtration through a weighed Whatman No. 1 filter paper. The filtrate was then evaporated to dryness to recover the unused silicone. The percent stationary phase was corrected accordingly. The columns were equilibrated at 250°C with helium flow for 20 hr to bleed the low boiling impurities. Presumably, the bulk of liquid was condensed to a uniform depth around the contact points between beads, as prescribed by Littlewood (32).

Chromatographic Procedure

A Hamilton 1.0 μl and a 2.5 μl syringe were used for sample

injection. For low boiling point samples, a small sample size of around 0.02 μl was used; for high boiling point, a sample of about 2.5 μl was used. Width at half-height of the sample peak was measured with a Keufel and Esser ruler. The peak maximum was eye-balled and the air peak was the unretained peak. The elution process was timed with a timer with an accuracy of 0.05 sec. A 250°C thermometer with an accuracy of 0.1° was used to monitor the temperature of the gas chromatograph, and a temperature fluctuation of ± 1°C was found. Noises and vibration of the gas chromatograph were observed during the analysis of Viscasil-100,000 and DC-550.

A description of the column characteristics is shown in Table 2.

Calculations

The diffusivities were determined from the dispersion of samples in columns of stationary phase supported on glass beads as in equation (13). The diffusivity at unit pressure D_{g1} was calculated from the formula of Fuller, Schettler and Giddings (33).

$$D_{AB} = \frac{1.00 \times 10^{-3}\, T^{1.75}\, (1/M_A + 1/M_B)^{1/2}}{p\left[(\Sigma_A\, \nu_i)^{1/3} + (\Sigma_B\, \nu_i)^{1/3}\right]^2} \qquad (19)$$

where D_{AB} = binary diffusion coefficient, cm^2/sec

T = temperature, $^{\circ}K$

p = pressure, atm

M_A, M_B = molecular weight, g/mole

ν_i = special diffusion parameters to be summed over atoms, groups, and structural features of the diffusing species

$\frac{D_{AB}}{T^{1.75}}$ = D_o is tabulated for all the diffusants in Table 3.

The obstruction factor, γ, was assumed to be 0.73 (34). The density of the glass beads ρ_g was found to be 2.936, identical to the previous result (25, 35). The densities and coefficients of expansions of the polydimethylsiloxanes were obtained from the literature of General Electric Company; that of DC-550, DC-710 from Dow Corning Corporation literature; and OV-210, OV-225, and SP-2401 from Ohio Valley Specialty Chemical Company. Densities of silicones at higher temperature were extrapolated, using the corresponding coefficients of expansion.

Sufficiently high velocities were used so that any error in the first term of equation (13) would be negligible and sufficient stationary phase (0.3%) was used that gas phase mass transfer was negligible. The validity of the method was confirmed by Hawkes (25).

V. RESULTS AND DISCUSSION

Diffusion Coefficients

Experimental results of diffusion in silicones are shown in Tables 4-12. Diffusion data with partition coefficients less than 30 are discarded for the following reason. Low boiling point samples were quickly vaporized once injected into the chromatographic column and could easily diffuse backward into the septum, in the opposite direction to the flow of carrier gas. This extra dispersion caused erroneous diffusion data since equation (13) does not include instrumental contributions.

Methylsilicones

As shown in Tables 4-7, diffusion coefficients of organic compounds are considerably higher in high molecular weight dimethylsilicones than in lower ones. This is especially true of n-alkane diffusants. Chromatographic peaks for n-alkanes in methylsilicones become increasingly skewed as the molecular weight of the n-alkane increases and also as the molecular weight of the methylsilicone increases, as investigated in this work.

All these anomalies become small at high temperature, or even perhaps non-existant. There seems to be a transition temperature

between anomalous and regular behavior at around 150°C, as shown in Tables 6-7 and Figures 4-5. At about 200°C diffusion coefficients are higher in SF-96-2000 than in more viscous Viscasil-100,000. Indeed, the non-linear substances such as benzene, and chloroform reveal yet another anomaly in that in SE-30 they diffuse more slowly than the n-alkanes while in SF-96-2000, SF-96-200 and Viscasil-100,000 they diffuse faster, as shown in Tables 4-5.

Suspecting that the SE-30 may be distributed on the beads in a different way to the less viscous methylsilicones, the loaded beads were examined microscopically. As in the cases of Viscasil-100,000 and SF-96-2000, the SE-30 was confirmed to be collected at the contact points of the beads as annular rings. It may be that rather more of the SE-30 was distributed on the bead surface than with the lighter methylsilicones, but it would not be sufficient to account for the results in Tables 4-7.

Possible explanations for the anomalies are:

1. Rheological properties of polymers of sufficiently high molecular weight reveal a strong rigidity and the appearance of long relaxation time due to chain entanglements (36). The effects observed are an abrupt increase in viscosity dependence on molecular weight and the onset of a rubbery region. The precise nature of entanglements is not yet known. The critical entanglement molecular weight (the molecular weight at which

there is a sharp increase in the slope of the viscosity-molecular weight curve) of methylsilicone is 29, 600 g/mole (36). The molecular weights of SE-30 and Viscasil-100, 000 are well above it while that of SF-96-200 is below it. The relationship between viscosity and average molecular weight at viscosities above 10, 000 cp applies (37):

$$\log \eta = 3.6 \log \overline{M}w - 13.191 \qquad (20)$$

A similar model is adopted in this thesis for the SF-96 silicones with viscosities of 200, 500, and 1000 cp at 25°C. Commercial literature was used to achieve the following regression model which has a correlation coefficient of 0. 951 (38):

$$\log \eta = 1.8198 \log \overline{M}w - 4.9677 \qquad (21)$$

The calculated average molecular weight of SF-96-2000 is 34, 975.

The diffusion coefficient may be more concentration-dependent at high molecular weight than at lower ones. There is no obvious reason to suspect this, but it would account for the skewing of the peaks. The diffusion coefficients were determined by gas chromatography with diffusion sample sizes of the order of 0. 1 μl and columns containing around 0. 3 ml of polymer. Concentration dependence of diffusion in the polymers could be expected for a short length of the column. At low temperatures the dependence of diffusion coefficient on diffusant concentration of the magnitude mentioned above becomes

sharper. Even if the sample sizes may be regarded as small for gas chromatography they may still not be zero in concentration.

2. The free volume of the higher polymers may be greater. There is actually evidence for this in the data on densities of polydimethylsiloxane (mol. wt. $\sim 10^5$) (45) and DC-200 (20). It would account for the increased diffusion coefficients of higher molecular weight methylsilicones. The comparison of the free volume of the two silicones will be discussed in detail in the Philosophy chapter.

3. The anomaly revealed by the aromatic substances as compared to straight chain n-alkanes may be a direct clue to the role of critical entanglement molecular weight of methylsilicones in the diffusion process. Diffusion process of the aromatic substances in entangled polymers could very well be hindered by the entangled strands whereas the straight chain n-alkanes could easily go through the narrow "holes." Diffusion of these n-alkanes is believed to occur preferentially along the direction of greatest length of the molecule, which tends to penetrate the polymer with the penetrant oriented as a needle (39). Chain hydrocarbons are thought to diffuse by first penetrating with one segment into a "hole" when one of significant size is formed, followed by more segments when the hole has been sufficiently enlarged by thermal fluctuations. For methylsilicones of low

molecular weights the diffusion process of aromatic molecules may be faster because there is no polymer entanglement and for linear n-alkanes the diffusion is slower because it takes time for a longer molecule to go through the "hole."

Phenylsilicones

Diffusion coefficients in phenylsilicones are tabulated in Tables 8-12. Phenylsilicones with phenyl content of 25, 50 and 75% with increasing molecular weight were investigated and the experimental results show that diffusion coefficients are higher in the lower percent phenylsilicones than in the higher percent phenyl. Diffusion coefficients of non-linear substances are generally higher than the long n-alkanes. Chromatographic peaks for n-alkanes in the phenylsilicones also become increasingly skewed as the molecular weight of the n-alkane increases. In addition, there exists an anomaly with diffusion in OV-25, as compared to phenylsilicones with lower phenyl content. At low temperature, the author has found asymmetric G. C. peaks on OV-25, but normal peaks at temperatures above 150°C. This exactly parallels the findings of Butler and Hawkes (35). They found asymmetric peaks in SE-30 at temperatures below 150°C but good peaks with General Electric's SF-96-200. The author has also found good chromatographic peaks with SF-96-2000 and Viscasil-10^5 at 50-250°C range. The asymmetry in both cases is with high

molecular weight, extremely viscous polymers. The viscosity has been suspected to be the cause of the anomaly.

Fluorosilicones

The (3, 3, 3 trifluoropropyl) methylsilicones of OV-210 and SP-2401 which is chemically the same as OV-210 but with a lower viscosity, are studied and the results are listed in Tables 8-12. Diffusion coefficients in OV-210 are slightly higher than in SP-2401 and diffusion coefficients of aromatic substances such as benzene, toluene and isomeric xylenes are higher than the n-alkanes of slightly higher molecular weight than the aromatic compounds studied. All chromatographic peaks of both silicones at low temperature ($50^{\circ}C$) are asymmetric, but good peaks are obtained at high temperatures (100°-$250^{\circ}C$).

Cyanosilicone

Only OV-225, cyanopropylmethyl-phenylmethylsilicone, is investigated. All chromatographic peaks in OV-225 are asymmetric at $50^{\circ}C$, similar to other high molecular weight silicones, such as OV-25. Diffusion coefficients of aromatic substances studied in OV-225 are higher than the n-alkanes.

Partition Coefficients

Methylsilicones

Partition coefficients of n-alkanes in the methylsilicones are independent of the molecular weights of the silicones studied, according to Tables 4-7. For a particular substance, its partition coefficients in the methylsilicones at the temperature studied are approximately identical. Partition coefficients are proportional to the exponent of the carbon chain lengths of the n-alkanes, i.e., partition coefficients are higher for longer n-alkanes than shorter n-alkanes because of the larger van der Waals' forces of attraction. As in Tables 4-7, diffusion coefficients of longer n-alkanes are lower than shorter n-alkanes. The relation between diffusion coefficients and partition coefficients of n-alkanes in methylsilicones at temperatures of 50-200^{o}C is shown in Figures 2-5. The double log plots of diffusion coefficients against partition coefficients of n-alkanes reveal yet another anomaly. In Figures 2 and 3, the SE-30 lines plunge steeply with increasing carbon number at 50^{o} and 100^{o}C. These lines flatten out at 150^{o} and 200^{o}C, in the manner similar to the other methylsilicone curves, as shown in Figures 4 and 5.

In addition, at 198^{o}C, the SF-96-2000 line surpasses the Viscasil-10^{5} curve in comparison with the results at lower temperatures. The discussed anomaly adds to the mystery of the diffusion

process in methylsilicones as mentioned in the Results discussion section. There is no apparent relationship between diffusion coefficients of non-linear substances and partition coefficients in the silicones as shown in Tables 4-12. This may be explained by the fact that diffusion coefficients are of kinetic origin while partition coefficients are of thermodynamic origin. There is no reason to believe that kinetic rates could be predicted by their thermodynamic properties.

Phenylsilicones

Partition coefficients in phenylsilicones are lower in OV-25 than in DC-550 and DC-710, with the partition coefficients in the latter two silicones of similar magnitude. This is especially true for the n-alkanes, as shown in Tables 8-12.

Fluorosilicones

Partition coefficients in fluorosilicones of OV-210 and SP-2401 are such that the partition coefficients in the latter are higher than in the former. This deduction is made by the fragmentary information at the temperature range of 50°-250°C.

Cyanosilicone

Partition coefficients of OV-225 are considerably lower than in the less polar methylsilicones and phenylsilicones. This is expected

because the solubility of non-polar substances is higher in non-polar silicones than in more polar silicones. The partition coefficients in OV-225 are higher than in OV-210. This may be due to the fact that OV-225 has stronger dipoles (the dipoles of C ≡ N is 3.6 D, while that of C - F is 1.51 D). The difference in partition coefficients in the case of aromatic compounds is even more profound and this may be attributed to the higher polarizability of aromatics.

VI. PHILOSOPHY

Diffusion in Polydimethylsiloxanes

Translational Friction Coefficients and Comparison with Monomeric Friction Coefficients of Polymer Segments

The friction coefficients for translatory motion of diffusants in a polymer can be calculated by the relation

$$\zeta_1 = k\ T/D \tag{22}$$

where ζ_1 = translational friction coefficient, dyn sec/cm

k = Boltzmann constant, erg/^{o}K

D = diffusion coefficient, cm^2/sec

The translational friction coefficient may be compared with the friction coefficient per monomer unit, ζ_o. The monomeric friction coefficients for unentangled polydimethylsiloxanes (PDMS) can be calculated as follows, as suggested by Barlow et al. (40).

$$\zeta_o = 18\ \eta\ M_o^2 / a^2 N_o\ \rho \overline{M}n \tag{23}$$

where η = viscosity of PDMS in poise

M_o = monomeric molecular weight, 75 g/mole for PDMS

a^2 = mean square end-to-end distance per monomer unit, cm^2

N_o = Avogadro's number, 6.0225×10^{23} $mole^{-1}$

ρ = density, g/cm^3

$\overline{Mn}$ = number-average molecular weight, g/mole

For a polymer with pronounced entanglement, ζ_o is suggested by Plazek et al. (41) as

$$\zeta_o = \frac{36\eta M}{\rho N_o a^2 Z^2 (M/2Me)^{2.4}} \qquad (24)$$

where M = molecular weight, g/mole

Me = molecular weight between coupling entanglements, 17,600 g/mole for PDMS

Z = degree of polymerization, M/M_o

Monomeric frictional coefficients of PDMS at 51°C are calculated by the author from the above equations, taking $a^2 = 39.4\ (\text{Å})^2$ as suggested by Flory, Mandelkern, Kinsinger and Shultz (42). The translational friction coefficients for benzene in PDMS at 51°C are also calculated by the author from the experimental data from this work. The monomeric frictional coefficients and the translational friction coefficients are compared in Table 13.

The calculated ζ_o at 51°C for the PDMS are compatible with the results obtained by Chen and Ferry (43) for the PDMS cross-linked by high energy electrons, 8.91×10^{-9} dyn sec/cm at 25°C, and by Plazek et al. for PDMS (mol. wt. 4.1×10^5) with a ζ_o of 5.01×10^{-8} dyn sec/cm at 25°C.

An attempt has been made to correlate the diffusion coefficients of benzene in PDMS with the monomeric friction coefficients of PDMS. Tanner (44) measured the diffusion coefficients of 10% by weight of benzene in 90% by weight of PDMS by nmr spin echo, using a pulsed-field gradient. He found that the diffusion coefficient of benzene is sensitive to low polymer molecular weight (around 166 g/mole), but is insensitive to high molecular weight (4898-42, 658 g/mole). The double log plot of diffusion coefficient and molecular weight of Tanner's data is plotted along with the author's own data in Figure 10.

The log D vs. log $\overline{M}w$ plot levels off between $\overline{M}w$ 4, 898 and 42, 658. These agree with the limiting maximum monomeric friction coefficient of PDMS with $\overline{M}w$ 3.16×10^4 to 4.2×10^4, as suggested by Barlow (40), which is 9.0×10^{-9} dyn sec/cm at 30°C.

The data collected by the author at $\overline{M}w$ 11, 000 and 34, 975 seem to follow the same pattern of Barlow's data, but only to deviate positively at very high molecular weight. The explanation for this anomaly is unknown.

One clue is that Plazek et al. have found evidence of linkages of a quasi-permanent network in the molecular weights of 2.2×10^6 to 4.9×10^6 region. For PDMS of $\overline{M}w$ 4.1×10^5 the quasi-permanent network does not appear, but there are coupling entanglements spread about five times more closely than the linkages of the quasi-permanent network.

A survey of the specific volume of PDMS is deemed necessary to shed some light on the subject of free volume of the PDMS. The specific volume ν_{sp} for PDMS of mol. wt. around 10^5 has been determined accurately over the temperature ranges of 20-200°C by Shih and Flory (45). The ratio of volume at temperature T to volume at 25°C of DC-200 with viscosity of 100 to 1000 centistokes is commercially available over the temperature range of -10° to 140°C (20). The differential of ratio of specific volume at temperature T to specific volume at 25°C with respect to temperature for the two PDMS is compared in Figure 11. There is a drastic difference in the slopes of the two curves where the higher molecular weight PDMS curve increases sharply. There seems to be a sudden change of slope at about 100°C for the higher mol. wt. PDMS, but for the lower mol. wt. PDMS, the change of slope is at 55°C. The specific volume of the 10^5 mol. wt. PDMS is slightly higher than that for the DC-200, as indicated from Tables 14 and 15. This may very well account for the higher diffusion coefficients in Viscasil-10^5 than for the SF-96 silicones.

Diffusion in Phenylsilicones, Fluorosilicones, and Cyanosilicones

Diffusion in the phenyl-, fluoro-, and cyanosilicones is dictated by the size of the substituent groups. As shown in Tables 8-12 and Figures 6-9, the rate of diffusion in the silicones can be

arranged according to the steric hindrance of the silicones. The order of diffusion rate in the silicones, as deduced from the diffusion coefficients of n-alkanes at 150° and 200°C, is as the following:

DC-550 > OV-210 > SP-2401 > DC-710 > OV-225 > OV-25

It follows that diffusion is fastest in a silicone consisting of small organofunctional groups. The effect of steric hindrance is again reflected by the diffusion coefficients of isomeric xylenes, the order of which is:

para-xylene > meta-xylene > ortho-xylene

For other aromatics the order of diffusion coefficients in all the silicones studied is:

benzene > toluene > cyclohexane

VII. STATISTICAL LINEAR REGRESSION MODELS FOR DIFFUSION OF n-ALKANES IN SILICONES

An attempt has been made to relate diffusion coefficients to an Arrhenius equation

$$D_s = D_s^* \exp(-E_D/RT) \tag{25}$$

where D_s = diffusion coefficient in the polymeric stationary phase, cm^2/sec

D_s^* = pre-exponential factor

E_D = activation energy of diffusion, kcal/mole

Accordingly, a fit was attempted to the general equation, as suggested by Butler and Hawkes (35)

$$\ln D_s = (K_0 + K_1 C) - (K_2 + K_3 C) / RT \tag{26}$$

where K_{0-3} are constants and C is the carbon number of the n-alkanes. Results for the silicones are shown in Table 16. The correlation coefficient for the individual polymer is greater than 0.98 except for SE-30, SF-96-200 and OV-210, for which the largest number of data points were collected. However, the same general regression model when applied to the data of all the silicones gave a correlation coefficient of 0.7744. This means that the regression model is able to explain 59.97% of the variation of the entire data set. A

theoretical $\ln D_s$ against experimental $\ln D_s$ plot is shown in Figure 12.

It was suggested by Frisch (46) that the ratio of activation energies for diffusion of penetrants i and j in a polymer P was roughly constant, independent of the nature of the polymer P . In addition, the ratio of activation energies for diffusion of penetrant i in a pair of polymers P and P_o was also approximately constant, independent of the penetrant i employed. The constancy of these ratios suggests the activation energies E_D for diffusion can be factored into a product of two functions, the first function g(i) characterizing solely the penetrant i, and the second function h(P) characterizing solely the polymer P; i. e. ,

$$E_D (i, P) = g(i)\, h(P) \tag{27}$$

The function g(i) increases with increasing size of the penetrant molecule (46). For n-alkanes, this would mean the chain length and may very well be represented by the carbon number of the n-alkanes.

A survey of the activation energy for diffusion from the regression model in Table 16 reveals that the experimental data are in line with the above argument.

The second function h(P), governed by the intermolecular and intramolecular potential energy of the polymer chain, is difficult to assess because the internal pressure is often unavailable for polymeric

materials. The author uses an empirical parameter density, which is known for all polymers, to correlate with the function h(P).

From Figure 13, the diffusion coefficients of n-dodecane, n-undecane and p-xylene in DC-550, DC-710 and OV-25 at about 150°C are strongly dependent on the percent phenyl content of the silicones. It seems intuitively sound to include the percent phenyl content of the silicones in the Arrhenius equation. The pre-exponential term D_s^* is defined as

$$D_s^*(i, P) = g(i) + h^*(P) \tag{28}$$

where g(i) is the carbon number of the n-alkanes, and $h^*(P)$ is the percent of phenyl content in the polymer. The regression model is thus

$$\ln D_s = (K_0 + K_1 C + K_2 \%_p) - (K_3 + K_4 C d) / RT \tag{29}$$

where K_{0-4} = constants

d = density of the polymer at temperature T, g/cm^3

$\%_p$ = percent phenyl in polymer

R = gas constant, 1.98717 cal/°K mole

T = temperature, °K

The validity of the regression model was tested with the data of the silicones. A correlation coefficient of 0.7431 was obtained, i.e., the regression model explained 55.2% of the variation.

A slightly different version of the above regression model was tested for the entire data set.

$$\ln D_s = (K_0 + K_1 C + K_2 \%_p) - (K_3 + K_4 C + K_5 d) / RT \qquad (30)$$

A correlation coefficient of 0.9053 was obtained, or 82% of the variation was explained by the regression model. The inclusion of partition coefficients in equation (30) did not improve the correlation coefficient (0.9053). The plot of theoretical $\ln D_s$ against experimental $\ln D_s$ is shown in Figure 14. The regression equations are shown in Table 17.

VIII. COMMENTS ON THE DETERMINATION OF DIFFUSION COEFFICIENTS BY GAS-LIQUID CHROMATOGRAPHY

The chromatographic method of determination of diffusion coefficients has the advantage that data on a wide range of diffusants can be collected over a wide temperature range in a short time. A quantitative determination of diffusion coefficient D_s requires firstly that the only significant source of peak spreading be due to slow equilibration through the stationary phase. A second requirement for interpretation of the C_1 term is that the geometry of the stationary phase should be well-defined, so that a good estimate of the depth of the polymeric liquid pool may be obtained. The depth of the pool has not been determined precisely in this work. A suspicion has been that the frontaling of chromatographic peaks of long n-alkanes at low temperatures is due to non-linear isotherm relating vapor and stationary phase concentrations of diffusants. The instrumental dead volume could also contribute extra dispersion.

Comparisons of diffusion coefficients with those obtained using conventional techniques (47) are complicated by the different areas of applicability of the methods. At any given temperature, the gas chromatographic method gives results with small concentrations of diffusants of rather low volatility than is usual in sorption or permeation experiments (48). Moreover, the G. C. method gives no handle

on concentration-dependent diffusion coefficients. Thus for comparison, data at zero diffusant concentration were required for systems where the polymer, diffusant and temperature range were convenient for gas chromatography. The little data available (43, 44) confirm the validity of the method.

BIBLIOGRAPHY

1. James, A. T. and A. J. P. Martin. Gas-liquid partition chromatography: the separation and microestimation of volatile fatty acids from formic acid to dodecanoic acid. Journal of Biochemistry 50:679-690. 1952.

2. Brandt, W. W. Small molecule diffusion in cold-drawn on stretched polymer films. Journal of Polymer Science 41:415-423. 1959.

3. Brandt, W. W. and G. A. Anysas. Diffusion of gases in fluorocarbon polymers. Journal of Applied Polymer Science 7:1924. 1963.

4. Warrick, E. L., M. J. Hunter and A. J. Barry. Polymer chemistry of the linear siloxanes. Industrial and Engineering Chemistry 44:2198. 1952.

5. Roth, W. L. The possibility of free rotation in the silicones. Journal of the American Chemical Society 69:474-475. 1947.

6. Roth, W. L. and D. Harker. The crystal structure of octamethylspiro[5.5]pentasiloxane: rotation about the ionic silicon-oxygen bond. Acta Crista 1:34-42. 1948.

7. Scott, D. W. Equilibria between linear and cyclic polymers in methylpolysiloxanes. Journal of the American Chemical Society 68:2294-2298. 1946.

8. Speier, J. L. Chloromethylmethylpolysiloxanes. Journal of the American Chemical Society 71:273-274. 1949.

9. Wilcock, D. F. Liquid methylsiloxane systems. Journal of the American Chemical Society 69:477-487. 1947.

10. Pauling, L. Nature of the chemical bond. Ithaca, New York, Cornell University Press, 1948.

11. Harney, N. B. and C. P. Smyth. The dipole moment of hydrogen fluoride and the ionic character of bonds. Journal of the American Chemical Society 68:171-173. 1946.

12. Trash, C.R. Methylsilicones--Their chemistry and use as a gas chromatographic liquid phases. Journal of Chromatographic Science 11:197. 1973.

13. Coleman, A.E. Chemistry of liquid phases--Other silicones. Journal of Chromatographic Science 11:200. 1973.

14. Haken, J.K. Polysiloxane stationary phases. Journal of Chromatography 73:442. 1972.

15. Rotzsche, H. Gas chromatography, ed. by M. van Swaay. London, Butterworth, 1962. 111 p.

16. Rotzsche, H. and Institute for Silicon and Fluorocarbon Chemistry. British Patent 1, 018, 800.

17. Technical Data Book. General Electric Company. Silicone Products Department, Waterford, New York.

18. Commercial Literature. Ohio Valley Specialty Chemical Company, Marietta, Ohio.

19. Thrash, C.R. Ohio Valley Specialty Chemical Company, Marietta, Ohio. Personal communication, June 28, 1973.

20. Commercial Literature. Dow Corning Corporation, Midland, Michigan.

21. Giddings, J.C. Dynamics of chromatography. Part I. New York, Marcel Dekker, Inc., 1965.

22. Giddings, J.C. General combination law for C_1 terms in gas chromatography. Journal of Physical Chemistry 68:186-187. 1964.

23. Giddings, J.C. Lateral diffusion and local nonequilibrium in gas chromatography. Journal of Chromatography 5:61-67. 1961.

24. Knox, J.H. Evidence for turbulence and coupling in chromatographic columns. Analytical Chemistry 38:253-261. 1966.

25. Hawkes, S.J., C.P. Russell and J.C. Giddings. Test of the theory of glass bead columns in gas liquid chromatography. Analytical Chemistry 37:1523-1526. 1965.

26. Giddings, J. C. Plate height contributions in gas chromatography. Analytical Chemistry 33:962-963. 1961.

27. Giddings, J. C. Comparison of theoretical and experimental efficiencies in glass bead gas chromatography columns. Analytical Chemistry 34:1026-1027. 1962.

28. Giddings, J. C. Liquid distribution on gas chromatographic support. Analytical Chemistry 34:458-459. 1962.

29. Giddings, J. C. Advance in the theory of plate height in gas chromatography. Analytical Chemistry 35:442-443. 1963.

30. Nyberg, D. G. An investigation of column efficiency and the relationship to liquid phase distribution on ultra-low loaded glass bead gas chromatographic columns. M. S. thesis. Salt Lake City, Utah, Brigham Young University, 1968. 110 numb. leaves.

31. Hawkes, S. J. and D. G. Nyberg. Column parameters for ultra-low loaded glass bead columns in gas chromatography. Analytical Chemistry 41:1613-1614. 1969.

32. Littlewood, A. B. Gas chromatography. New York, Academic Press, 1958. 23 p.

33. Fuller, E. N., P. D. Schettler and J. C. Giddings. A new method for prediction of binary gas-phase diffusion coefficients. Industrial and Engineering Chemistry 58:20-21. 1966.

34. Hawkes, S. J. Obstruction factors are flow sensitive. Analytical Chemistry 44:1296-1297. 1972.

35. Butler, L. and S. J. Hawkes. Diffusion in long-chain solvents. Journal of Chromatographic Science 10:518-519. 1972.

36. Porter, R. S. and J. F. Johnson. The entanglement concept in polymer systems. Chemical Reviews 66:14-15. 1966.

37. Martellock, A. C. Silicone Products Department, General Electric Company, Waterford, New York. Personal communication, July 9, 1969.

38. Sober, H. F. Silicone Products Department, General Electric Company, Waterford, New York. Personal communication, June 21, 1971.

39. Smith, T. G. Review of diffusion in polymer penetrant systems. 1968. 21 p. (University of Maryland. College Park, Maryland. For the National Aeronautics and Space Administration. NASA Contract No. NGR-20-022-053)

40. Barlow, A. J., G. Harrison and J. Lamb. Viscoelastic relaxation of polydimethylsiloxane liquids. Royal Society of London. Proceedings A282:244-248. 1964.

41. Plazek, D. J., W. Dannhauser and J. D. Ferry. Viscoelastic dispersion of polydimethyl siloxane in the rubberlike plateau zone. Journal of Colloid Science 16:101-126. 1961.

42. Flory, P. J., L. Mandelkern, J. B. Kinsinger and W. B. Schultz. Molecular dimensions of polydimethylsiloxanes. Journal of the American Chemical Society 74:3364-3367. 1952.

43. Chen, S. P. and J. D. Ferry. The diffusion of radioactively tagged n-hexadecane and n-dodecane through rubbery polymers. Effects of temperature, cross-linking, and chemical structure. Macromolecules 1:273-278. 1968.

44. Tanner, J. E. Diffusion in a polymer matrix. Macromolecules 4:748-750. 1971.

45. Shih, H. and P. J. Flory. Equation-of-state parameters for poly(dimethylsiloxane). Macromolecules 5:759-760. 1972.

46. Frisch, H. L. and T. K. Kwei. Factorization of the activation energies of diffusion of gases in polymers. Polymer Letters 7:789-790. 1969.

47. Crank, J. and G. S. Park. Diffusion in polymers. New York, Academic Press, 1968.

48. Gray, D. G. and J. E. Guillet. Studies of diffusion in polymers by gas chromatography. Macromolecules 6:226-227. 1973.

APPENDIX

Methylsilicones = SE-30, Viscasil-100,000, SF-96-2000, SF-96-200

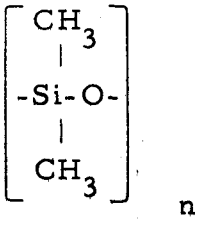

Phenylmethylsilicones = DC-550, DC-710

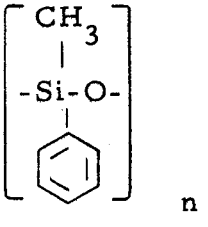

Phenylmethyldiphenylsilicone = OV-25

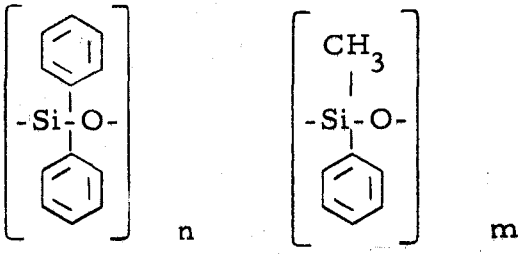

Trifluoropropylmethylsilicones = OV-210, SP-2401

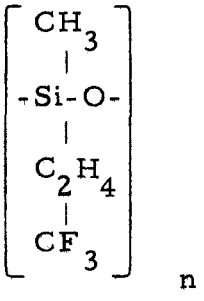

Figure 1. Structure of Silicones.

Cyanopropylmethyl-phenylmethylsilicone = OV-225

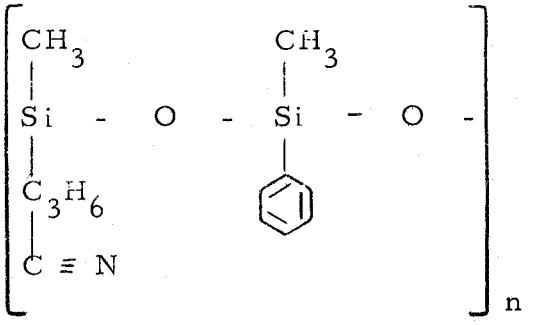

where n, m are non-zero positive integers.

Figure 1. (Continued)

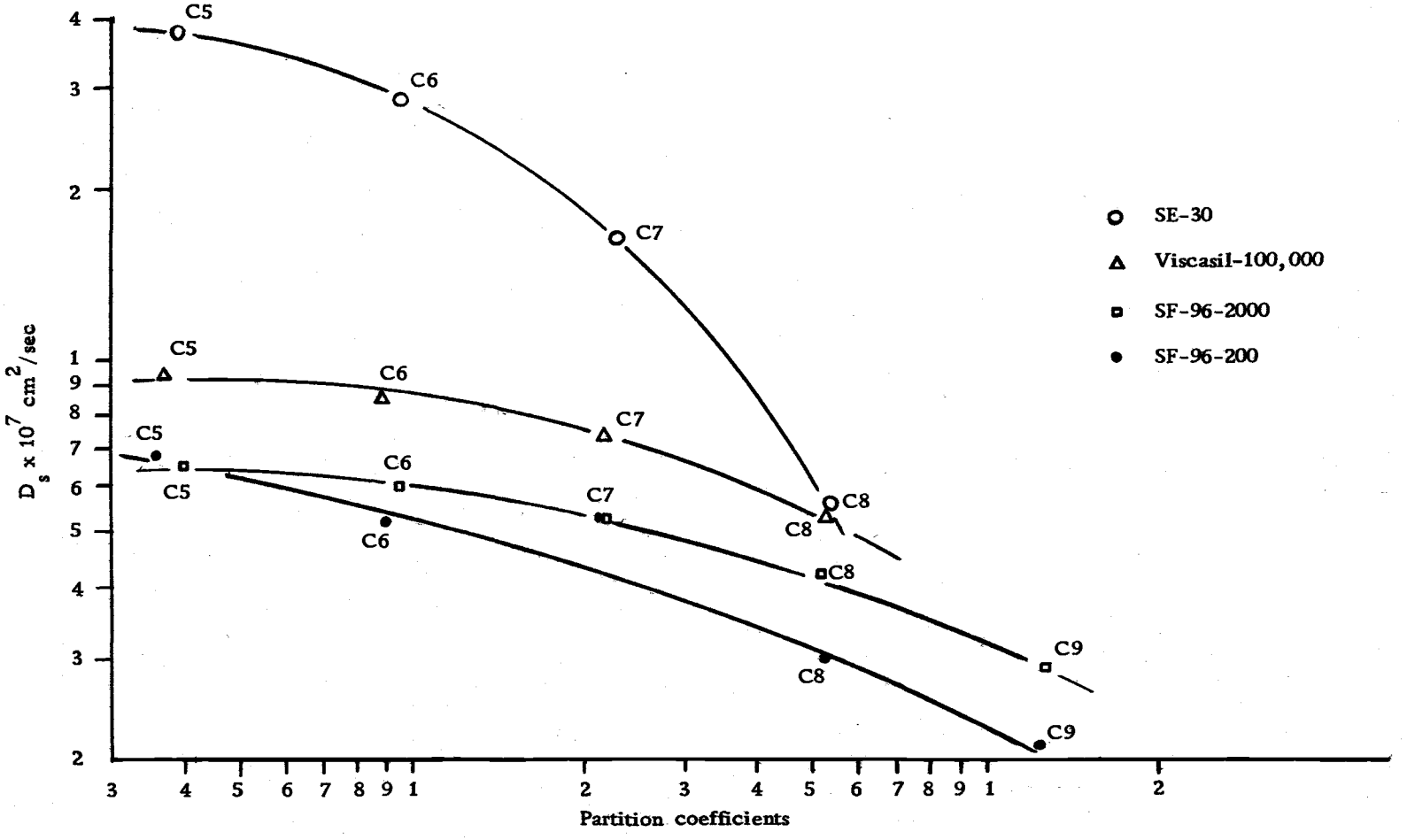

Figure 2. Log diffusion coefficients against log partition coefficients in methylsilicones at 50 ± 2°C.

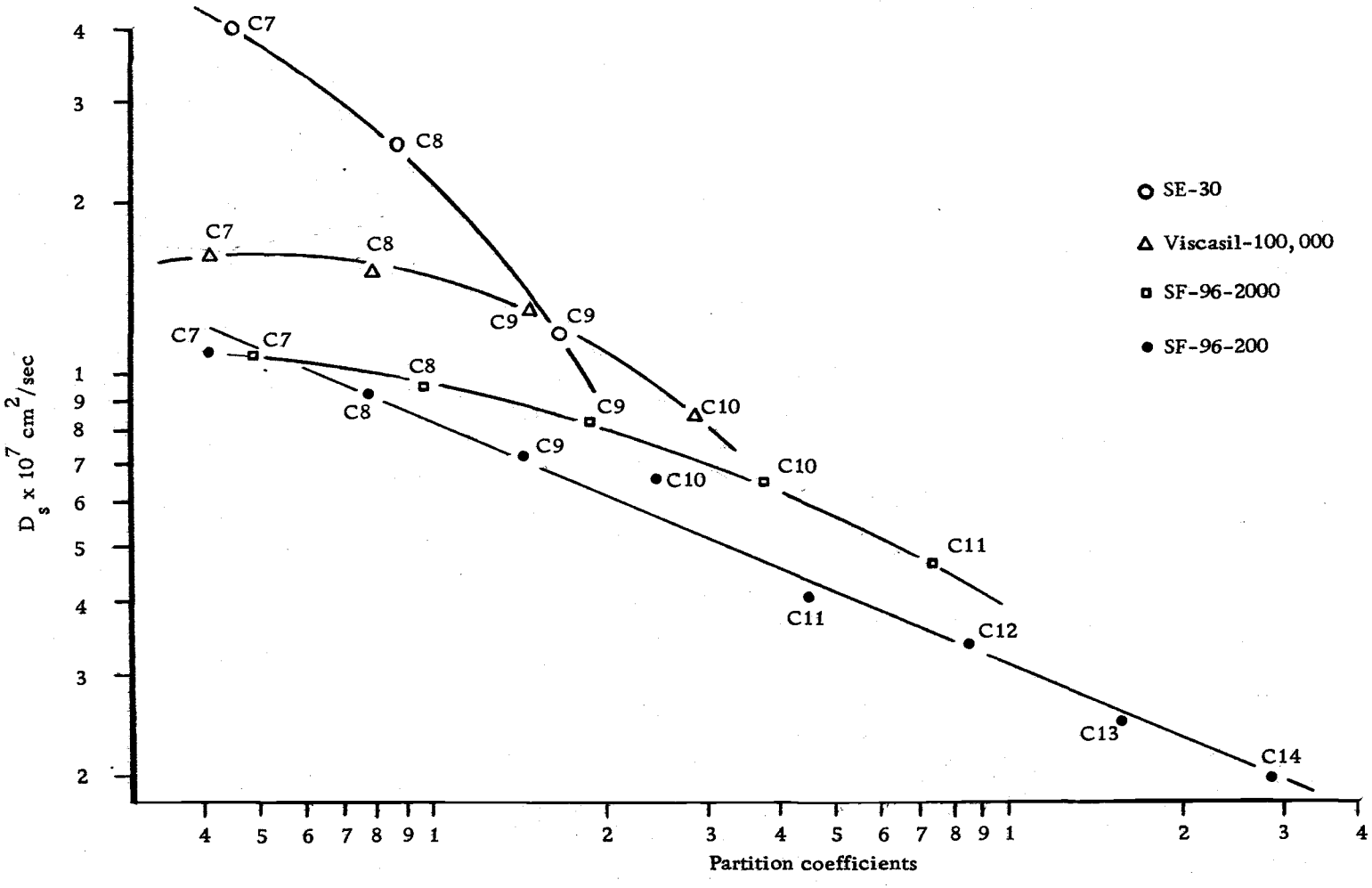

Figure 3. Log diffusion coefficients against log partition coefficients in methylsilicones at 99 ± 3°C.

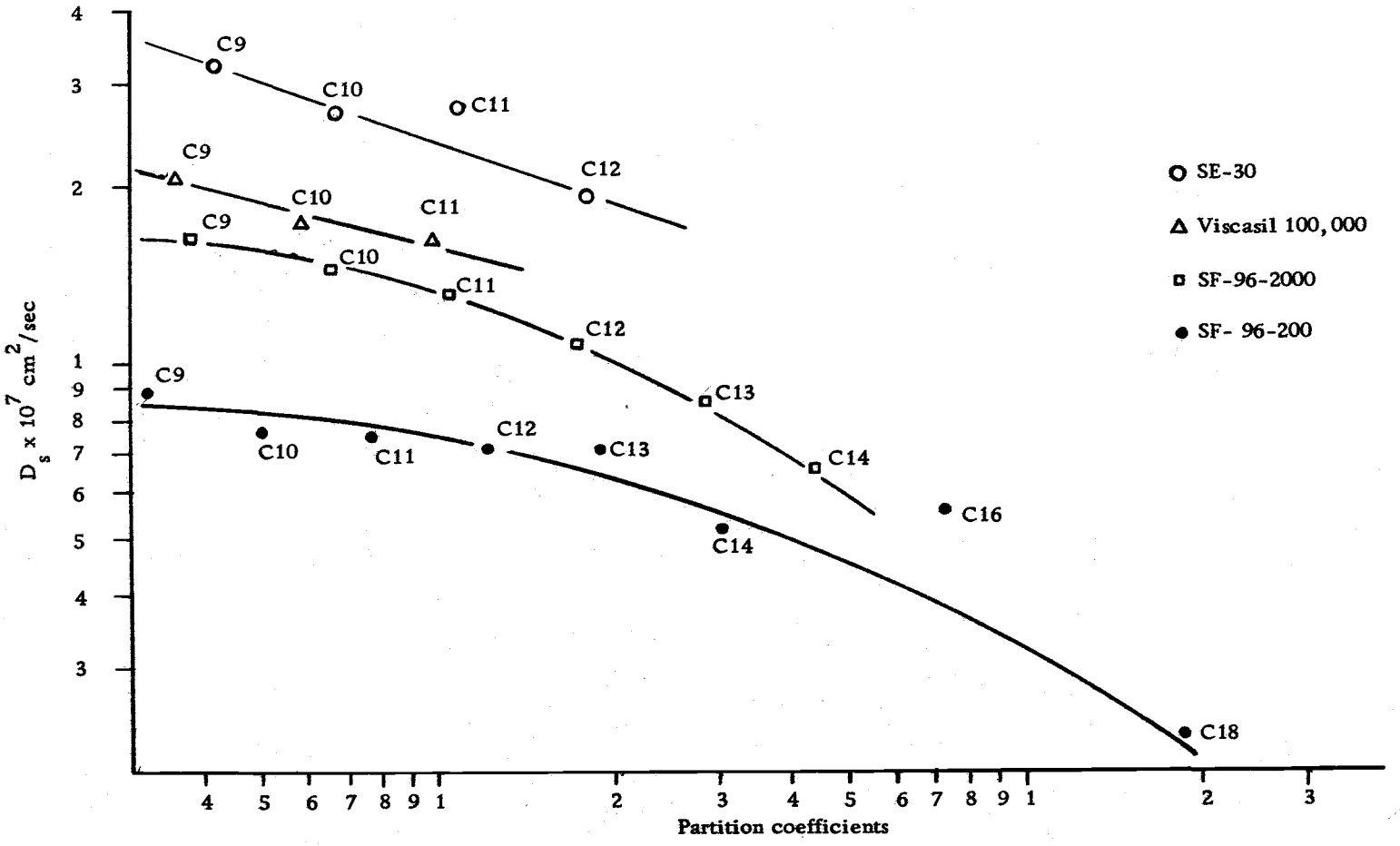

Figure 4. Log diffusion coefficients against log partition coefficients in methylsilicones at 148 ± 3°C.

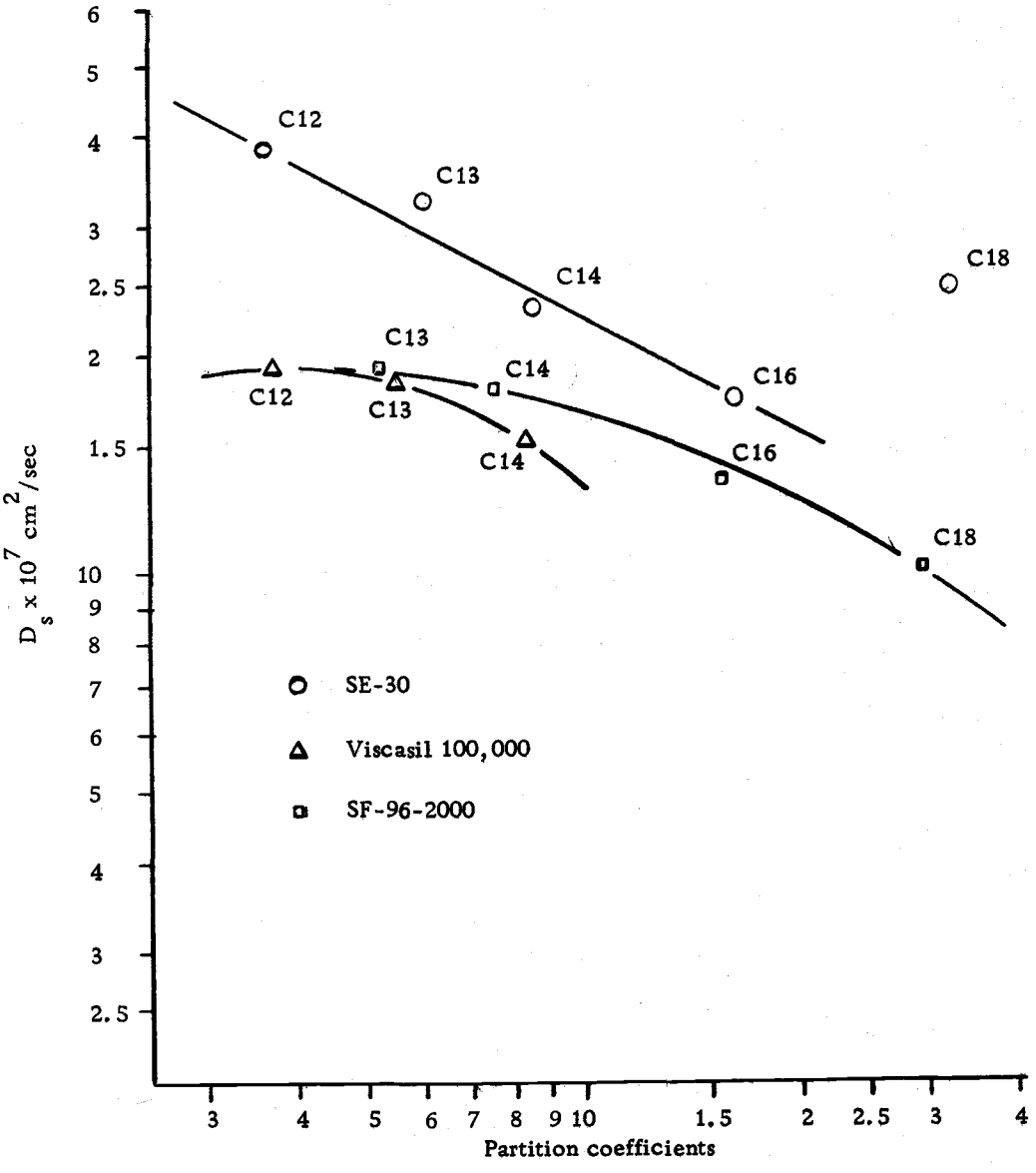

Figure 5. Log diffusion coefficients against log partition coefficients in methylsilicones at 197.8 ± 0.3°C.

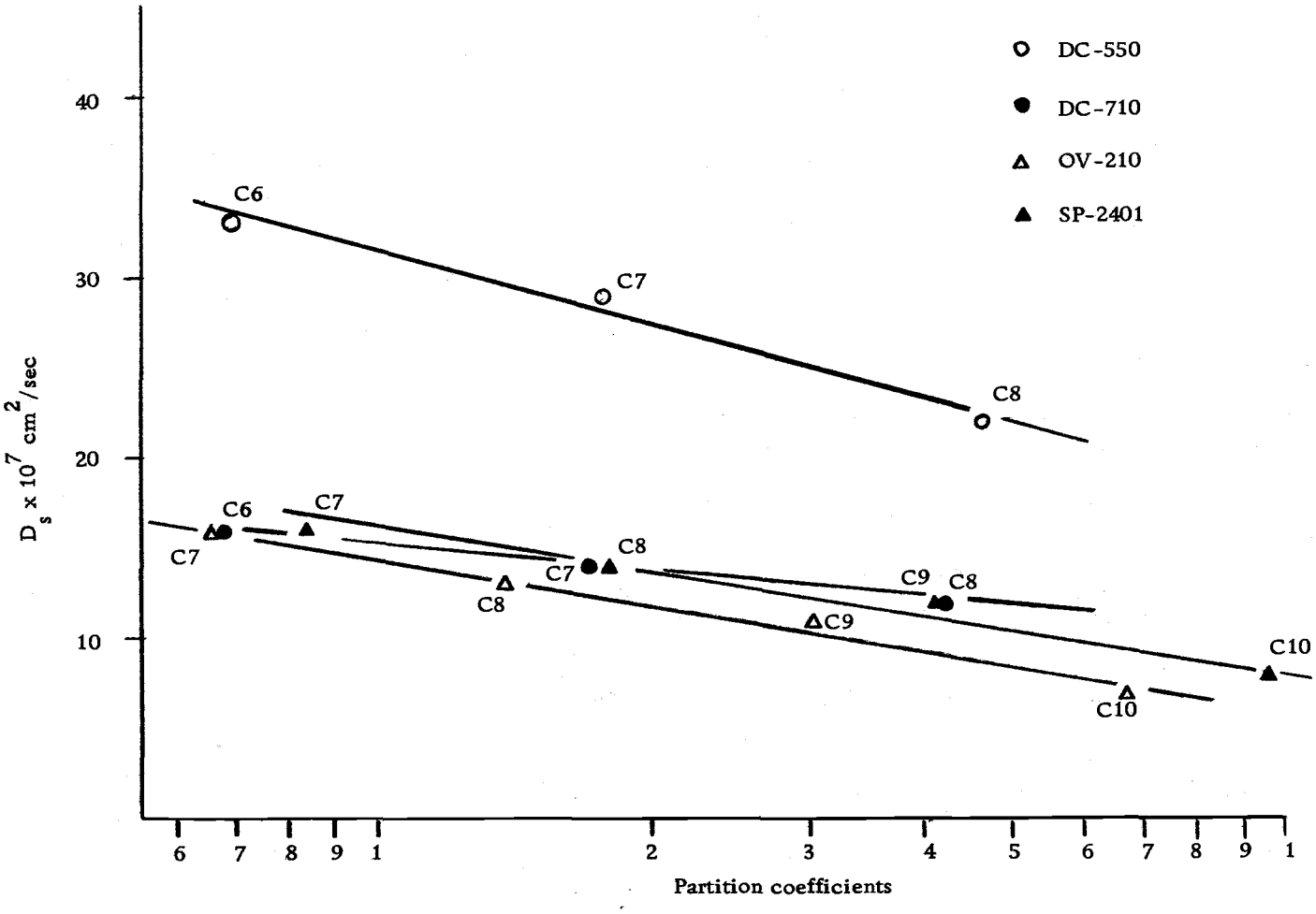

Figure 6. Diffusion coefficients against log partition coefficients in phenyl- and fluorosilicones at 49 ± 2°C.

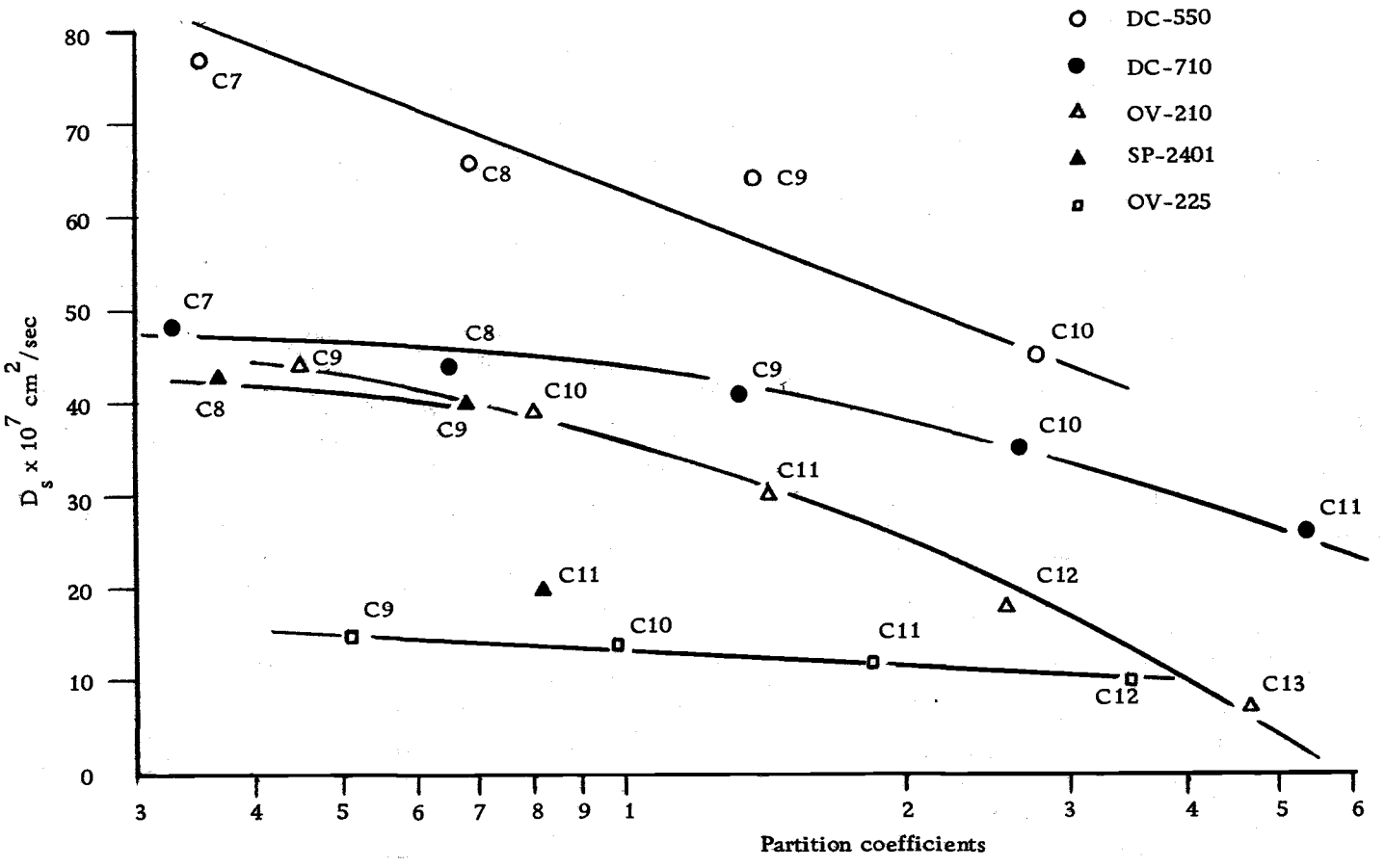

Figure 7. Diffusion coefficients against log partition coefficients in phenyl-, fluoro- and cyanosilicones at 98 ± 2°C.

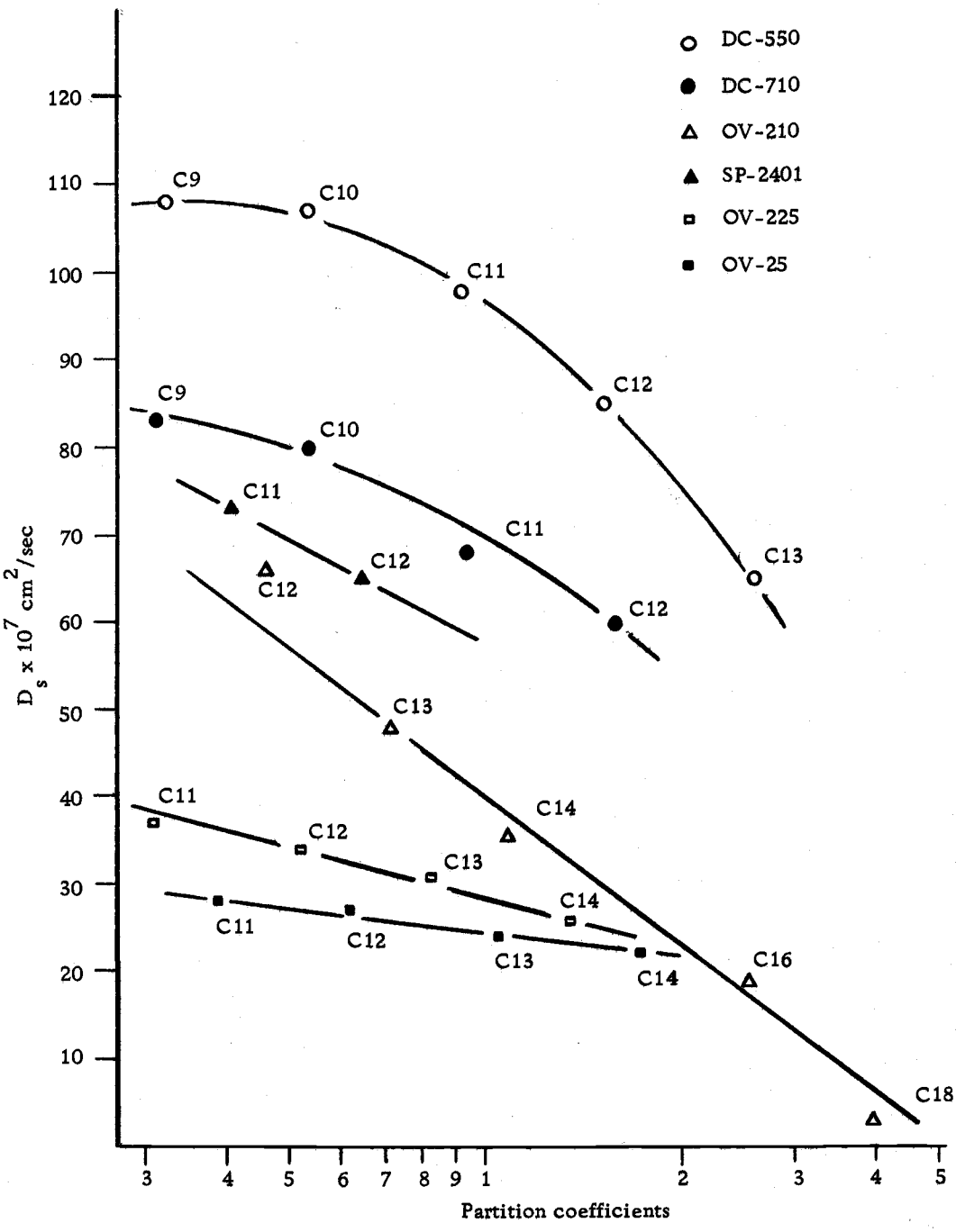

Figure 8. Diffusion coefficients against log partition coefficients in phenyl-, fluoro- and cyanosilicones at 149 ± 1°C.

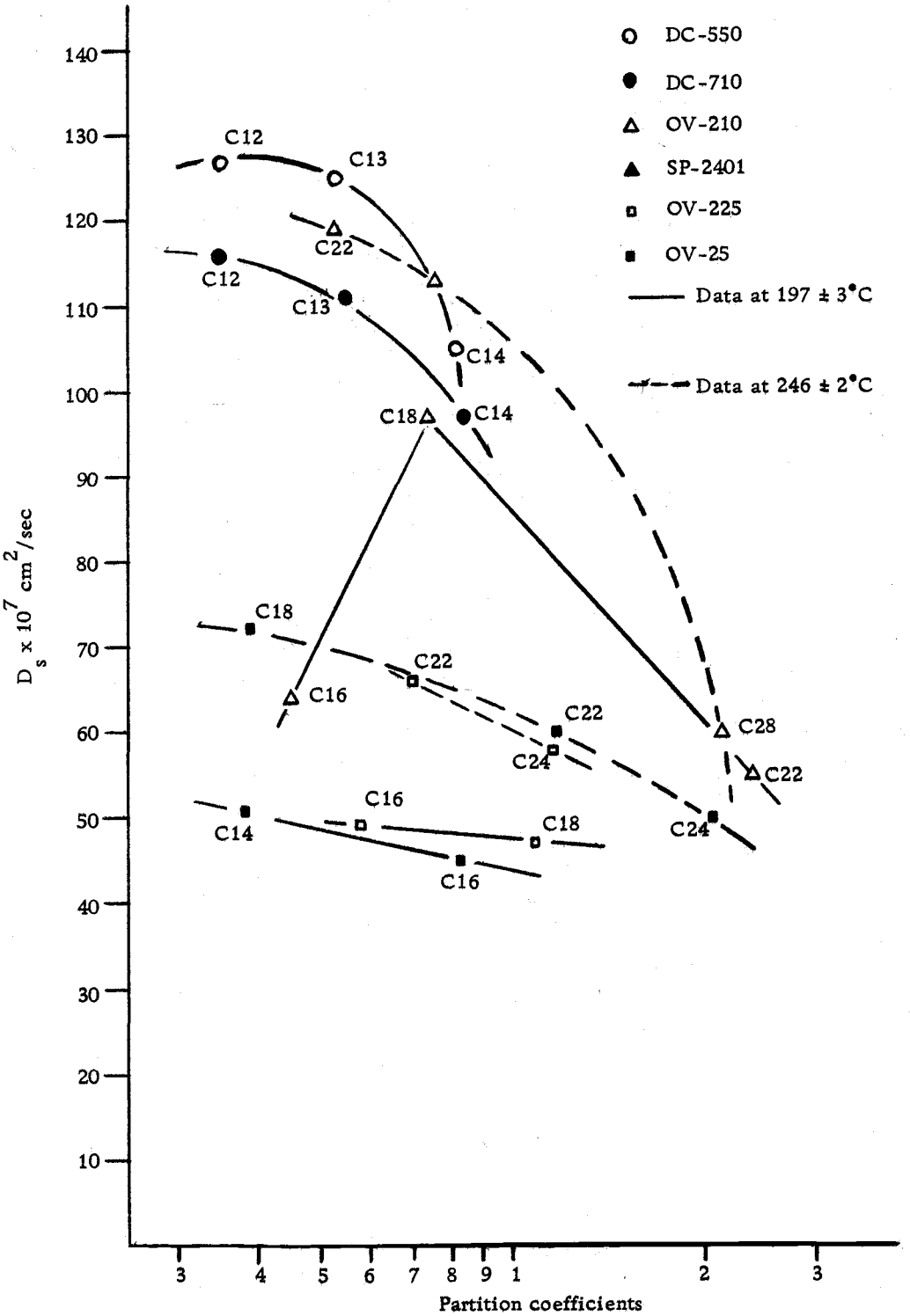

Figure 9. Diffusion coefficients against log partition coefficients in phenyl-, fluoro- and cyanosilicones at 197 ± 3°C and 246 ± 2°C.

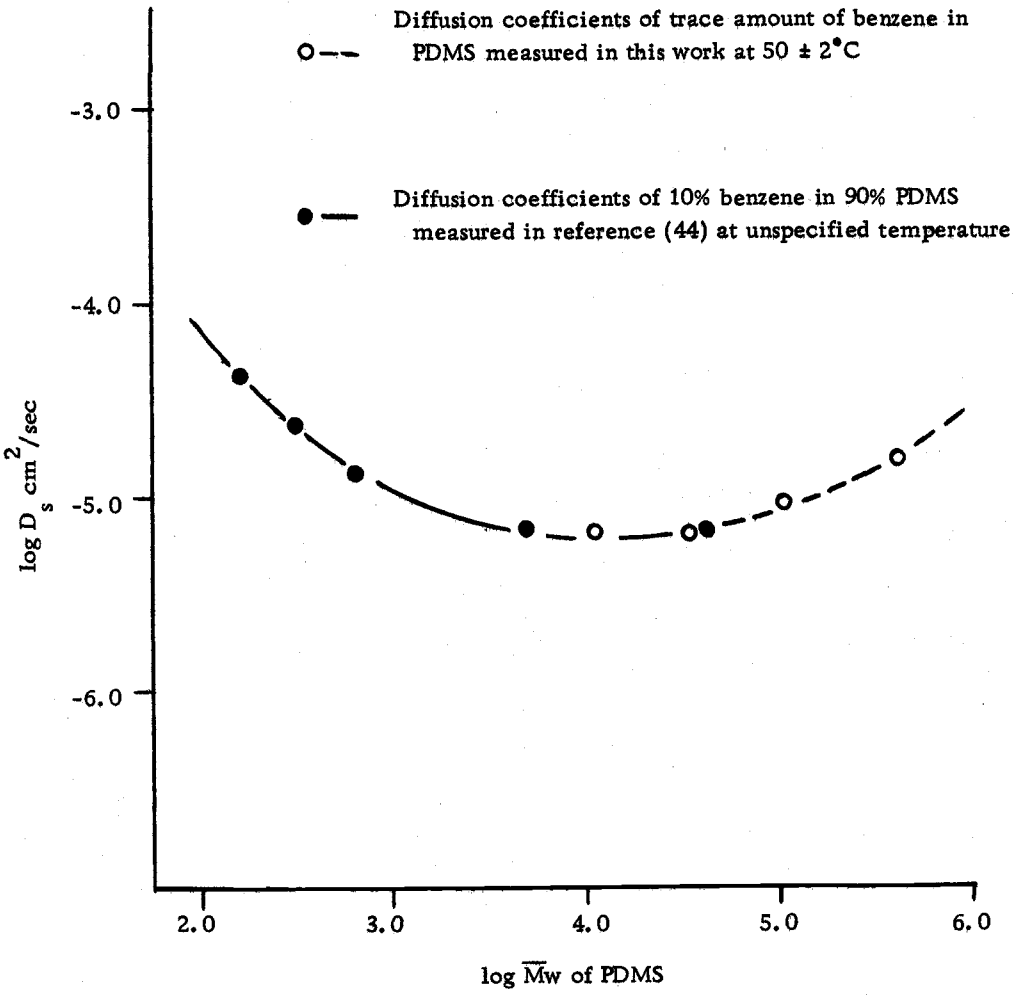

Figure 10. Diffusion of benzene in polydimethylsiloxanes.

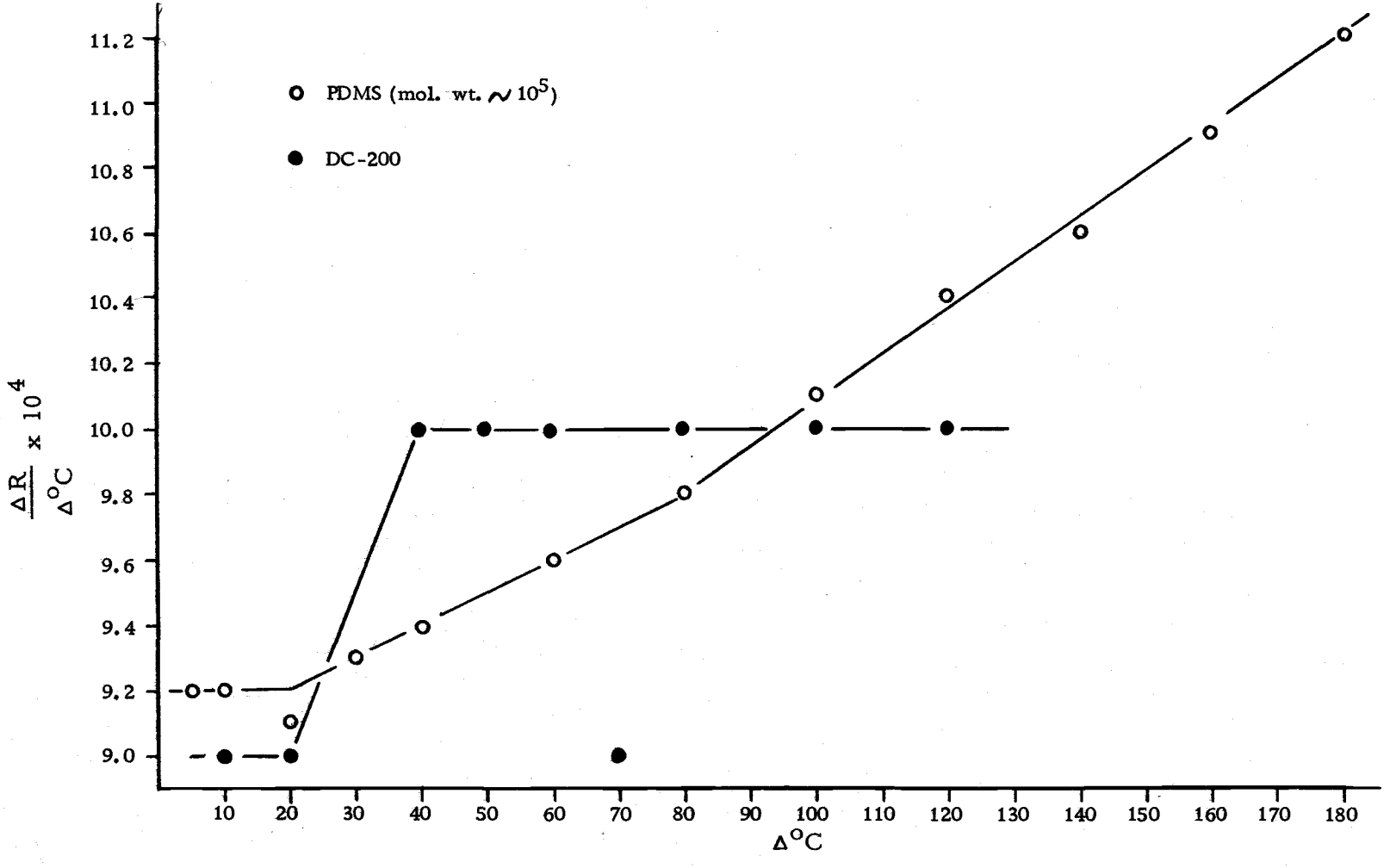

Figure 11. Differential of ratio of specific volume at temperature T to specific volume at 25°C with respect to temperature for PDMS (mol. wt. ~10^5) and DC-200.

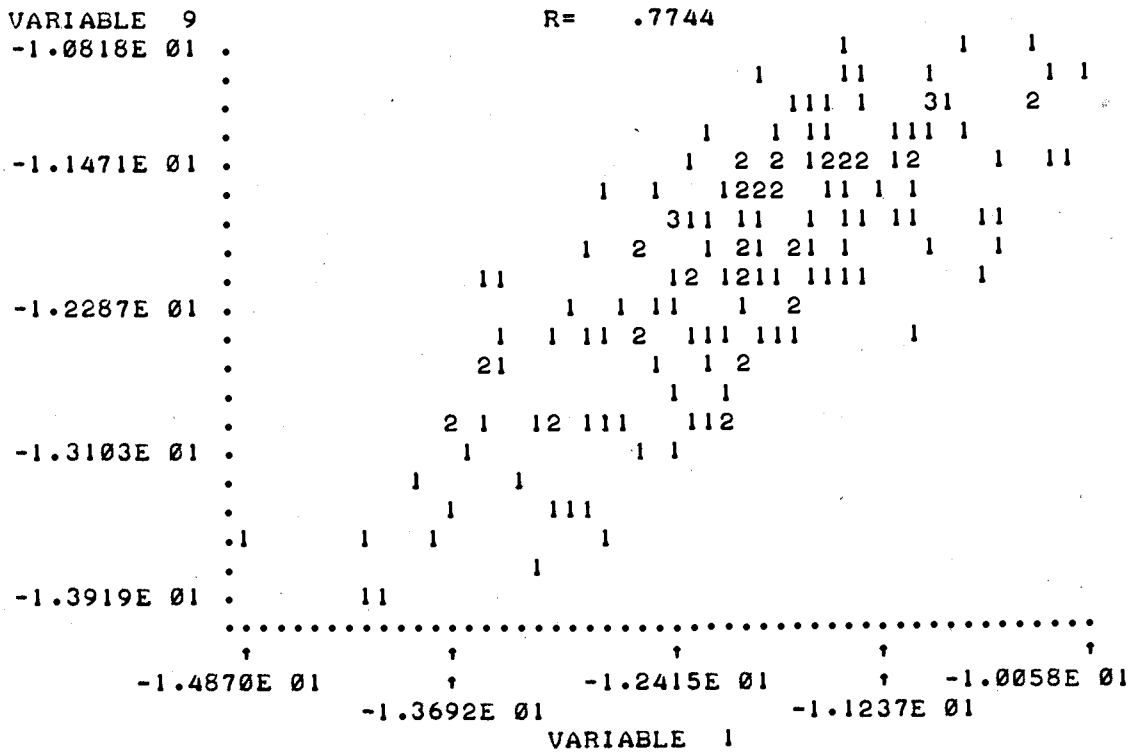

Figure 12. Theoretical ln D_s against experimental ln D_s--regression equation 26.

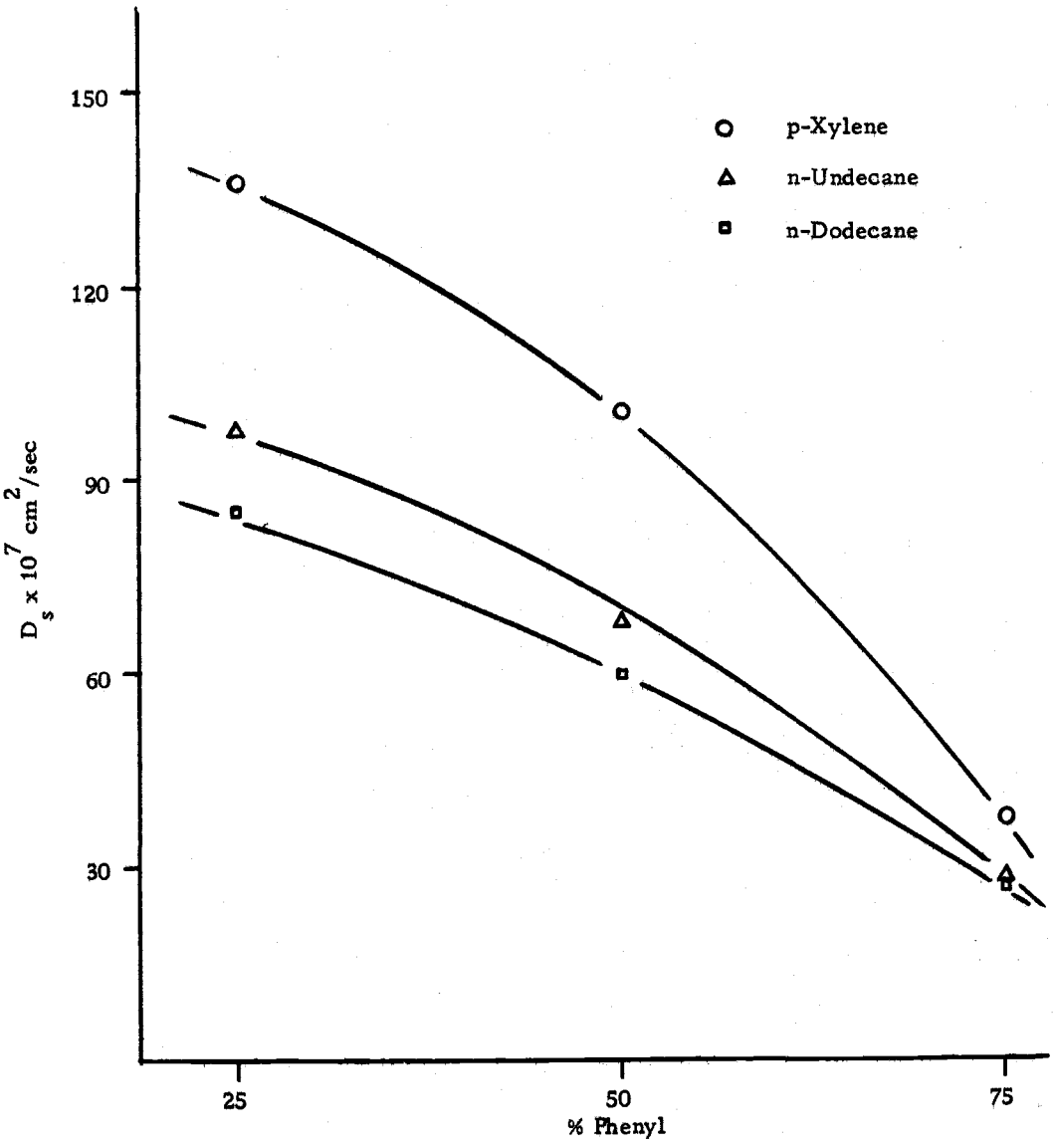

Figure 13. Diffusion coefficients against percent phenyl content of phenylsilicones at 140 ± 1°C.

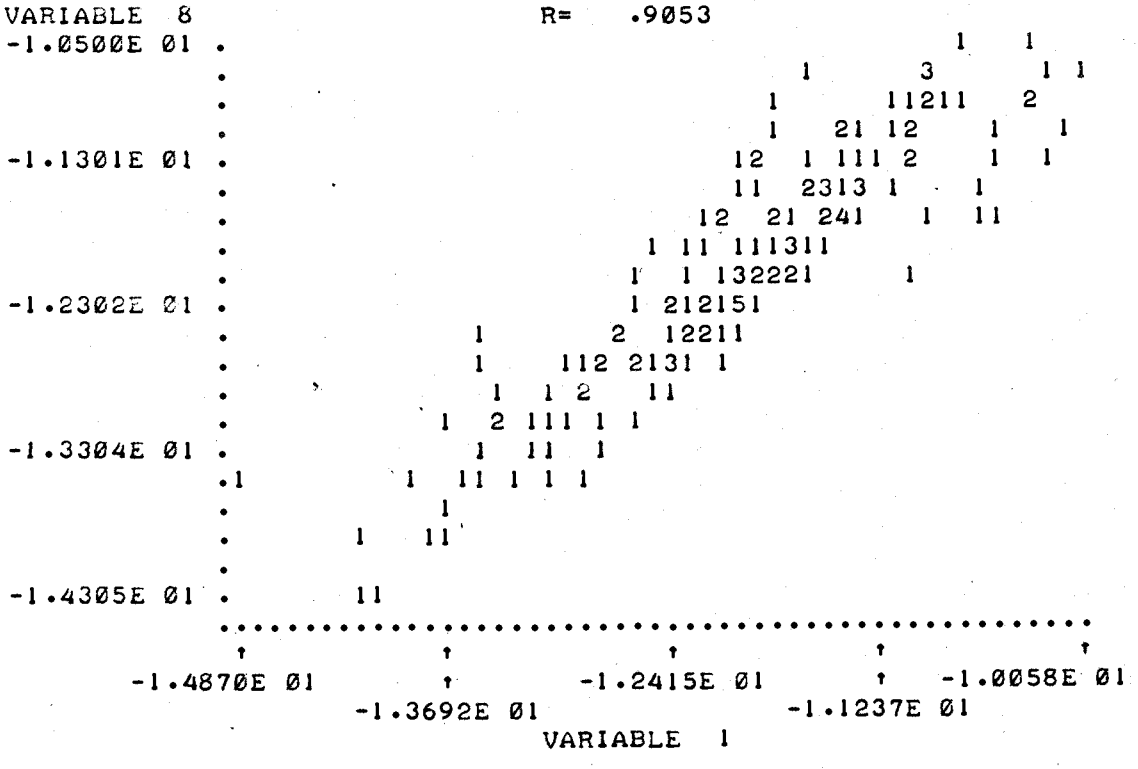

Figure 14. Theoretical ln D_s against experimental ln D_s--regression equation 30.

Table 1. Some properties of silicones.

	SE-30	Viscasil 100,000	SF-96-2000	SF-96-200	DC-550	DC-710	OV-25	OV-210	SP-2401	OV-225
Viscosity cts at 25°C	9.47×10^6	100,000	2,000	200	115	475-525	>100,000	10,000	700	9,000
Avg. mol. wt.	400,000	103,000	34,975	11,000		2,600	1×10^4	2×10^5		8×10^3
S. G. at 25°/25°C	0.966[a]	0.978	0.974	0.972	1.068	1.10	1.150	1.284	1.30	1.096
Coefficient of expansion[c] cc/cc/°C	9.25×10^{-4}	9.25×10^{-4}	9.25×10^{-4}	9.25×10^{-4}	4.2×10^{-4}[b]	4.3×10^{-4}[b]	4.3×10^{-4}[b]	9.5×10^{-4}	9.5×10^{-4}	8.0×10^{-4}
% Phenyl	0	0	0	0	25	50	75	0	0	25

[a] at 29.8°C

[b] cc/cc/°F

[c] 25-150°C

Table 2. Column characteristics.

Stationary phase	Column length (ft)	Column diameter (in. O. D.)	% Stationary phase	Solvent	Carrier gas	Temperature range (^{o}C)
SE-30	5. 97	3/16	0. 3110	ethyl acetate	helium	50-200
Viscasil-10[5]	5. 96	1/4	0. 2697	chloroform	helium	50-200
SF-96-2000	5. 91	1/4	0. 3338	chloroform	helium	50-200
SF-96-200	6. 0	3/16	0. 346	ethyl acetate	helium	50-150
DC-550	5. 91	1/4	0. 323	chloroform	helium	50-200
DC-710	7. 0	1/4	0. 307	chloroform	helium	50-200
OV-25	6. 0	1/4	0. 3896	acetone	helium	150-250
OV-210	6. 0	1/4	0. 3613	acetone	helium	50-250
SP-2401	5. 91	1/4	0. 3025	acetone	helium	50-250
OV-225	6. 0	1/4	0. 3129	acetone	helium	100-200

Table 3. D_o of n-alkanes and aromatics. $cm^2/sec/^oK$

	$D_o \times 10^5$		$D_o \times 10^5$
n-Pentane	1.353	n-Octadecane	0.678
n-Hexane	1.230	n-Docosane	0.606
n-Heptane	1.135	n-Tetracosane	0.576
n-Octane	1.057	n-Octacosane	0.529
n-Nonane	0.992	Chloroform	1.577
n-Decane	0.935	Carbon tetrachloride	1.417
n-Undecane	0.889	Cyclohexane	1.252
n-Dodecane	0.848	Benzene	1.776
n-Tridecane	0.812	Toluene	1.315
n-Tetradecane	0.782	Xylene	1.100
n-Hexadecane	0.724	Napthalene	1.020

Table 4. Diffusion coefficients in cm^2/sec and partition coefficients of n-alkanes and aromatics in methylsilicones at 50 ± 2°C.

	SF-96-200 (50.5°C)		SF-96-2000 (48°C)		Viscasil-10^5 (51°C)		SE-30 (51°C)	
	$D_s \times 10^7$	K	$D_s \times 10^7$	K	$D_s \times 10^7$	K	$D_s \times 10^7$	K
n-Pentane	68	36	65	40	94	37	377	39
n-Hexane	52	90	60	95	86	89	288	96
n-Heptane	53	212	53	218	74	218	163	229
n-Octane	30	525	42	516	53	533	56	539
n-Nonane	21	1238	29	1267				
Cyclohexane			41	163	58	153		
Benzene	66	139	68	154	98	143	156	161
Chloroform	73	92	72	100			338	102
Carbon tetrachloride			45	164	65	148		
p-Xylene					43	856		
m-Xylene	39	804			24	903		
o-Xylene					31	1032		
Toluene	53	349						

Table 5. Diffusion coefficients in cm^2/sec and partition coefficients of n-alkanes and aromatics in methylsilicones at 99 ± 3°C.

	SF-96-200 (100°C)		SF-96-2000 (94.5°C)		Viscasil-10^5 (102°C)		SE-30 (100°C)	
	$D_s \times 10^7$	K	$D_s \times 10^7$	K	$D_s \times 10^7$	K	$D_s \times 10^7$	K
n-Heptane	110	41	109	49	162	41	403	45
n-Octane	93	78	96	96	153	78	254	87
n-Nonane	72	144	83	189	130	149	119	165
n-Decane	66	246	65	372	85	285		
n-Undecane	41	452	47	717				
n-Dodecane	34	848						
n-Tridecane	25	1578						
n-Tetradecane	20	2846						
Cyclohexane			87	41	120	34		
Benzene	139	30	133	39	195	33	314	37
Chloroform								
Carbon tetrachloride			92	39	141	34		
p-Xylene			108	154	155	124		
m-Xylene	113	108	99	149	144	122		
o-Xylene			92	179	125	146		
Toluene	136	58	122	76			194	72
Napthalene	71	746						

Table 6. Diffusion coefficients in cm^2/sec and partition coefficients of n-alkanes and aromatics in methylsilicones at 148 ± 3°C.

	SF-96-200 (152.5°C)		SF-96-2000 (145°C)		Viscasil-10^5 (149°C)		SE-30 (146°C)	
	$D_s \times 10^7$	K	$D_s \times 10^7$	K	$D_s \times 10^7$	K	$D_s \times 10^7$	K
n-Nonane	89	32	163	38	207	36	324	42
n-Decane	76	50	147	66	175	59	269	67
n-Undecane	75	77	131	104	163	98	274	108
n-Dodecane	71	122	108	172			194	178
n-Tridecane	71	190	86	286				
n-Tetradecane	52	306	66	439				
n-Hexadecane	56	731						
n-Octadecane	23	1876						
Cyclohexane								
Benzene								
Chloroform								
Carbon tetrachloride								
p-Xylene			191	36	178	32		
m-Xylene			172	36	151	33	310	38
o-Xylene			165	40	150	38		
Toluene								
Napthalene	171	122	154	173			453	179

Table 7. Diffusion coefficients in cm^2/sec and partition coefficients of n-alkanes and aromatics in methylsilicones at 197.8 ± 0.3°C and 239°C.

	SF-96-2000 (198°C)		Viscasil-10^5 (198°C)		SE-30 (197.5°C)	
	$D_s \times 10^7$	K	$D_s \times 10^7$	K	$D_s \times 10^7$	K
n-Dodecane			193	37	388	36
n-Tridecane	193	52	184	55	324	60
n-Tetradecane	181	75	154	83	233	85
n-Hexadecane	135	155			176	161
n-Octadecane	102	295			250	321
Napthalene	263	41			620	41
	(239°C)					
n-Hexadecane	218	48				
n-Octadecane	187	83				
n-Docosane	113	258				

Table 8. Diffusion coefficients in cm^2/sec and partition coefficients of n-alkanes and aromatics in phenyl and fluorosilicones at $49 \pm 2^{\circ}C$.

	DC-550 (51°C)		DC-710 (49°C)		OV-210 (48°C)		SP-2401 (51°C)	
	$D_s \times 10^7$	K	$D_s \times 10^7$	K	$D_s \times 10^7$	K	$D_s \times 10^7$	K
n-Hexane	33	69	16	68				
n-Heptane	29	177	14	172	16	66	16	84
n-Octane	22	469	12	422	13	139	14	181
n-Nonane					11	302	12	414
n-Decane					7	671	8	960
Cyclohexane	23	149	10	153	11	54	12	65
Benzene	33	198	15	247	25	117	25	125
Chloroform	38	138	18	170	22	64	22	69
Carbon tetrachloride	24	172	10	197	13	64	15	73
Toluene					20	259	24	268

Table 9. Diffusion coefficients in cm^2/sec and partition coefficients of n-alkanes and aromatics in phenyl-, fluoro-, and cyanosilicones at 98 ± 2°C.

	DC-550 (100.5°C)		DC-710 (99°C)		OV-210 (97°C)		SP-2401 (97°C)		OV-225 (97.5°C)	
	$D_s \times 10^7$	K	$D_s \times 10^7$	K	$D_s \times 10^7$	K	$D_s \times 10^7$	K	$D_s \times 10^7$	K
n-Heptane	77	35	48	33						
n-Octane	66	68	44	65			43	37		
n-Nonane	64	137	41	133	44	45	40	68	15	51
n-Decane	45	276	35	267	39	80			14	98
n-Undecane			26	534	30	143	20	82	12	183
n-Dodecane					18	255			10	348
n-Tridecane					7	463				
Cyclohexane	66	33	38	33						
Benzene	92	40	57	47			80	31	24	42
Chloroform	91	30	57	34					19	38
Carbon tetrachloride	69	37	40	42						
p-Xylene	70	164	47	186	59	87	56	99	19	143
m-Xylene	65	164	44	192	52	89	49	102	17	144
o-Xylene	57	201	39	235	46	111	46	126	15	187
Toluene					66	50	63	56	20	78

Table 10. Diffusion coefficients in cm^2/sec and partition coefficients of n-alkanes and aromatics in phenyl-, fluoro- and cyanosilicones at 149 ± 1°C.

	DC-550 (149°C)		DC-710 (150°C)		OV-25 (148°C)		OV-210 (149°C)		SP-2401 (149°C)		OV-225 (148°C)	
	$D_s \times 10^7$	K	$D_s \times 10^7$	K	$D_s \times 10^7$	K	$D_s \times 10^7$	K	$D_s \times 10^7$	K	$D_s \times 10^7$	K
n-Nonane	108	32	83	31								
n-Decane	107	53	80	53								
n-Undecane	98	91	68	93	28	39			73	41	37	31
n-Dodecane	85	151	60	159	27	62	66	46	65	65	34	52
n-Tridecane	65	257			24	104	48	71			31	82
n-Tetradecane					22	171	36	108			26	134
n-Hexadecane							19	255				
n-Octadecane							3	397				
p-Xylene	136	40	100	46	37	32					52	33
m-Xylene	127	40	91	46	31	33					45	33
o-Xylene	122	48	84	56	28	40					42	42
Napthalene					26	284	116	130			41	320

Table 11. Diffusion coefficients in cm^2/sec and partition coefficients of n-alkanes and aromatics in phenyl-, fluoro-, and cyanosilicones at 197 ± 3°C.

	DC-550 (198°C)		DC-710 (202°C)		OV-25 (195°C)		OV-210 (198°C)		SP-2401 (194°C)		OV-225 (197°C)	
	$D_s \times 10^7$	K	$D_s \times 10^7$	K	$D_s \times 10^7$	K	$D_s \times 10^7$	K	$D_s \times 10^7$	K	$D_s \times 10^7$	K
n-Dodecane	127	35	116	35								
n-Tridecane	125	53	111	55								
n-Tetradecane	105	82	97	84	51	38			100	38		
n-Hexadecane					45	83	64	45			49	58
n-Octadecane							97	74			47	109
n-Docosane							55	240				
Napthalene					67	72	183	32	164	46	86	72

Table 12. Diffusion coefficients in cm^2/sec and partition coefficients of n-alkanes and aromatics in phenyl-, fluoro- and cyanosilicones at 246 ± 2°C.

	OV-25 (245°C)		OV-210 (244°C)		SP-2401 (247°C)		OV-225 (247°C)	
	$D_s \times 10^7$	K	$D_s \times 10^7$	K	$D_s \times 10^7$	K	$D_s \times 10^7$	K
n-Octadecane	72	39						
n-Docosane	60	118	119	53	131	70	66	70
n-Tetracosane	50	209	113	76			58	115
n-Octacosane			60	214				
Napthalene							121	26

Table 13. Translational friction coefficients for benzene and monomeric friction coefficients for segmental motion.

Silicone	Viscosity at 51°C poise	ζ_1 at 51°C x 10^9 dyn sec cm^{-1}	ζ_o at 51°C x 10^9 dyn sec cm^{-1}
SF-96-200	0.126[a]	6.78	1.00
SF-96-2000	1.469	6.58	3.16
Viscasil-10^5	63.466	4.57	4.09
PDMS (mol. wt. 4.1 x 10^5)	43652[b]	2.87	25.8

[a]Data interpolated from General Electric Commercial Literature.

[b]Data interpolated from falling ball viscosity in reference 41.

Table 14. Ratio of specific volume at temperature T to specific volume at 25°C for PDMS (mol. wt. 10^5) at selected temperatures.[a]

Temperature (°C)	Ratio (R)	ν_{sp}	$\Delta R/\Delta$ °C
20	0.9954	1.0265	
			0.00092
25	1.0000	1.0312	
			0.00092
30	1.0046	1.0359	
			0.00091
40	1.0137	1.0453	
			0.00093
50	1.0230	1.0549	
			0.00094
60	1.0324	1.0646	
			0.00096
80	1.0516	1.0844	
			0.00098
100	1.0712	1.1046	
			0.00101
120	1.0913	1.1254	
			0.00104
140	1.1120	1.1467	
			0.00106
160	1.1332	1.1686	
			0.00109
180	1.1550	1.1910	
			0.00112
200	1.1773	1.2140	

[a]Data obtained from reference 45.

Table 15. Ratio of volume at temperature T to volume at 25°C for DC-200 at selected temperatures. [a]

Temperature (°C)	Ratio (R)	ν_{sp} [b]	Δ R/Δ°C
-10	0.967	0.9978	
			0.0008
0	0.975	1.0061	
			0.0010
10	0.985	1.0164	
			0.0009
20	0.994	1.0257	
			0.0009
30	1.003	1.0350	
			0.0009
40	1.012	1.0443	
			0.0008
50	1.020	1.0525	
			0.0010
60	1.030	1.0629	
			0.0010
70	1.040	1.0732	
			0.0010
80	1.050	1.0835	
			0.0009
90	1.059	1.0928	
			0.0010
100	1.069	1.1031	
			0.0010
120	1.089	1.1237	
			0.0010
140	1.108	1.1433	

[a] Data extracted from reference 46 for DC-200.

[b] The density of SF-96-200 at 25°C was used to calculate the specific volume of DC-200 at selected temperatures.

Table 16. Regression equations for diffusion coefficients of n-alkanes in individual silicone.

$$\ln D_s = K_o + K_1 C + (K_2 + K_3 C) / (RT)$$

(Std. error, T)

	K_o	K_1	K_2	K_3	R	N	F(1, N-4, 0.95)
SE-30	-9.046	0.5108	717.9	-621.7	0.8624	18	4.60
(SE, T)	(1.568, -5.8)	(0.1445, 3.5)	(1150.0.6)	(137.1, -4.5)			
Viscasil 100,000	-4.331	-0.1633	-4049	- 10.98	0.9832	14	4.96
(SE, T)	(0.8126, -5.3)	(0.075, -2.2)	(559.5, -7.2)	(59.9, -0.18)			
SF-96-2000	-6.084	0.0969	-2888	-212.2	0.9916	23	4.38
(SE, T)	(0.339, -17.9)	(0.027, 3.6)	(244, -12)	(24.8, -8.6)			
SF-96-200	-8.230	0.1952	-1392	-303.5	0.9293	21	4.45
(SE, T)	(1.567, -5.3)	(0.1590, 1.2)	(1148, -1.2)	(123.9, -2.4)			
DC-550	-4.139	-0.1393	-4833	- 15.61	0.9937	12	5.32
(SE, T)	(0.8779, -4.7)	(0.0833, -1.7)	(631.5, -7.7)	(69.6, -0.22)			
DC-710	-3.433	-0.1801	-5896	42.0	0.9971	15	4.84
(SE, T)	(0.6163, -5.6)	(0.057, -3.2)	(440.2, -13.4)	(45.4, 0.93)			
OV-210	-9.834	0.7947	1669.7	-951.1	0.9197	16	4.75
(SE, T)	(3.50, -2.8)	(0.2, 4.0)	(2826, 0.6)	(192.6, -4.9)			
OV-225	-4.323	0.0105	-5817	-102.7	0.9976	12	3.32
(SE, T)	(0.532, -8.1)	(0.038, 0.28)	(448.6, -13)	(39.3, -2.6)			
SP-2401	-6.153	0.2091	-3372.6	-303	0.9957	11	5.59
(SE, T)	(0.668, -9.2)	(0.059, 3.5)	(543.8, -6.2)	(59.5, -5.1)			
OV-25	-4.282	-0.0593	-6496	- 7.631	0.9977	9	6.61
(SE, T)	(0.879, -4.86)	(0.061, -0.97)	(841.5, -7.72)	(61.6, -0.12)			

Table 17. Regression equations for diffusion coefficients of n-alkanes in silicones.

$$\ln D_s = (K_o + K_1 C) + (K_2 + K_3 C) / RT$$

(std. error, T)

K_o	K_1	K_2	K_3	R	N	F(1, N-4, 0.95)
-7.397	0.4277	-1110.5	-578.2	0.7744	158	3.84
(0.912, -8.11)	(0.075, 5.70)	(691.2, -1.61)	(70.4, -8.21)			

$$\ln D_s = (K_o + K_1 C + K_2 \%_p) + (K_3 + K_4 C\ d) / RT$$

(std. error, T)

K_o	K_1	K_2	K_3	K_4	R	N	F(1, n-5, 0.95)
-2.236	-0.1455	-0.0149	-5976.1	-2.86×10^{-5}	0.7431	158	3.84
(0.827, -2.70)	(0.0526, -2.76)	(2.42×10^{-3}, -6.16)	(470.6, -12.7)	(4.32×10^{-5}, -0.66)			

$$\ln D_s = (K_o + K_1 C + K_2 \%_p) + (K_3 + K_4 C + K_5 d) / RT$$

(std. error, T)

K_o	K_1	K_2	K_3	K_4	K_5	R	N	F(1, N-6, 0.95)
-8.257	0.406	-0.01297	1283.8	-530.1	-1939.8	0.9053	158	3.84
(6.529×10^{-1}, -12.6)	(5.09×10^{-2}, 7.97)	(1.54×10^{-3}, -8.41)	(5.759×10^{2}, 2.229)	(4.85×10^{1}, -10.9)	(2.393×10^{2}, -8.105)			